BDX-613-1748 (Rev.)

BURRS PRODUCED BY TURNING

By L. K. Gillespie

Published December 1978

Topical Report

Prepared for the United States Department of Energy
Under Contract Number DE-AC04-76-DP00613.

Bendix Kansas City Division

DISCLAIMER

Printed in the United States of America

Available From the National Technical Information Service, U.S. Department of Commerce, 5285 Port Royal Road, Springfield, Virginia 22161.

Price: Microfiche $3.00
Paper Copy $6.00

BDX-613-1748 (Rev.)
Distribution Category UC-38

BURRS PRODUCED BY TURNING

By L. K. Gillespie

Published December 1978

Topical Report

L. K. Gillespie, Project Leader

Project Team:
B. J. Neal

Communications Services

Bendix Kansas City Division

BURRS PRODUCED BY TURNING

BDX-613-1748 (Rev.), Topical Report, Published December 1978

Prepared by L. K. Gillespie

Methods were determined for controlling turning-burr size to reduce deburring cost and improve the quality of miniature precision components. A maximum burr height and thickness of 25.4 μm (0.001 inch) are essential to obtaining consistent deburring and limiting stock loss to 2.54 μm (0.0001 inch) and edge radii to 76.4 μm (0.003 inch). Controlling factors include the tool's side-cutting edge angle, back rake, feedrate, and radial depth-of-cut, and the material's strain-hardening exponent and ductility.

WPC-pls

The Bendix Corporation
Kansas City Division
P. O. Box 1159
Kansas City, Missouri 64141

A prime contractor with the United States Department of Energy under Contract Number DE-AC04-76-DP00613

CONTENTS

ILLUSTRATIONS

TABLES

SUMMARY

Component parts of small precision mechanisms typically require edges that are free of burrs and nearly sharp to assure reliable operation of the mechanism. In the past, the reliable removal of machining burrs and the assurance of part-edge sharpness have dictated that deburring be performed only by hand. This method is inherently time-consuming and operator-variable.

Small burrs can be easily removed by many deburring processes. Because the repeatability of the deburring process and the time required for burr removal are directly related to the size of the burr, this study was initiated to determine how cutting conditions during turning operations affect the size of the burrs that are produced. The thickness and height of turning burrs produced from 303Se stainless steel; 15-5PH stainless steel; beryllium copper; glass sealing alloy, 53Fe-29Ni-17Co, SAE unified number K94610; and 2V permendur high magnetic permeability steel, 49Fe-49Co-2V, SAE unified number K95100 were studied. Theories of the formation of turning burrs also were developed.

Four different types of burrs occur on most turned parts. Depending upon how these burrs are produced, their properties differ significantly.

While increasing the feedrate and the radial depth-of-cut increase the burr size, decreasing the side-cutting edge angle and the rake angles increase the burr size more than any other factors. The strain-hardening exponent is the most significant material factor in determining the burr size, although workpiece ductility is also related.

To assure the removal of burrs from miniature precision parts while limiting the change in part size to 2.54 μm (0.0001 inch) and the final edge radii to 76.2 μm (0.003 inch), burr heights and thicknesses must be no greater than 25.4 μm (0.001 inch).

DISCUSSION

SCOPE AND PURPOSE

This study was undertaken to determine the influence of turning parameters upon the size of the burrs produced. Specifically, it sought to determine how feedrate, spindle speed, tool geometry, and workpiece geometry affect burr thickness and height.

PRIOR WORK

Although no previous work on turning burrs has been published by Bendix Kansas City, a brief analysis of burr heights produced by turning has been reported by this author elsewhere.[1] Related studies on burrs produced by reaming, ball-broaching, drilling, end-milling, side-milling, and grinding have been published by Bendix.[2-8] General theories concerning the formation of burrs also have been reported.[1,9-11]

ACTIVITY

All conventional machining operations produce burrs, the size of which depend on the tool geometries used, the speeds and feedrates, and the properties of the workpiece material.

The cost of burr removal is proportional to the burr size. In many instances, because of close tolerances, minute part size, and large burr size, the burr-removal cost for precision miniature parts may nearly equal the machining cost. To minimize these fabrication costs, the influence of machining conditions upon burr size and the influence of burr size upon burr-removal cost must be analyzed. A series of tests therefore have been initiated to provide data on burr properties as a function of machining conditions. These tests will include most of the common machining operations.

In this study of turning burrs, conceptual models of burr formation were developed and tests were performed which utilized five workpiece materials and a variety of cutting conditions.

Formation of Burrs During Turning Operations

In turning operations, burrs are formed by three basic mechanisms: a lateral flow of material (Poisson burr); chip roll-over (roll-over burr); and chip tearing (tear burr). Cutoff burrs, which are not true burrs involving plastic flow, also are produced on turned parts.

Poisson Burr

The Poisson burr is formed whenever the cutting edge of the tool extends beyond an edge of the workpiece (Figure 1). In essence, it is the lateral deformation that occurs whenever any solid is compressed. The term is derived from the fact that this burr is directly related to Poisson's ratio. The extent of the deformation is a function of the workpiece material, the size and shape of the contacting body, and the applied load.

In the case of a cutting tool in which no rubbing occurs on clearance surfaces, the effective shape of the indenter is a cylinder. Because cutting tools have cutting-edge radii of 5.08 to 127.0 μm (0.0002 to 0.0050 inch), the extent of the lateral deformation (burr size) also is relatively small. The actual size of the burr is proportional to the cutting-edge radius and the applied pressure. This can be shown through the use of a model of an infinitely small hole being expanded to have a radius equal to the cutting-edge radius. Using this burr-formation model provides the following relationships.

$$b_L = \left[\frac{b(1+\nu)\sigma_e e^{-\sqrt{3}\phi_a}}{\sqrt{3}E}\right]\left[-\frac{\sin\phi_\rho}{2\left(\sqrt{3}\cos\phi_\rho + \sin\phi_\rho\right)}\right], \quad (1)$$

$$b_t = r\left(e^{-\sqrt{3}\phi_a}\cos\phi_a - 1\right), \quad (2)$$

and

$$\phi_a = -\sin^{-1}\left(\frac{\sqrt{3}P}{2\sigma_e}\right) + \frac{\pi}{6}, \quad (3)$$

where

b_L = burr length (height),

b_t = burr thickness,

b = depth-of-cut in a turning operation,

ν = Poisson's ratio for elastic stresses,

σ_e = yield stress of a perfectly plastic material,

E = modulus of elasticity,

r = cutting-edge radius,

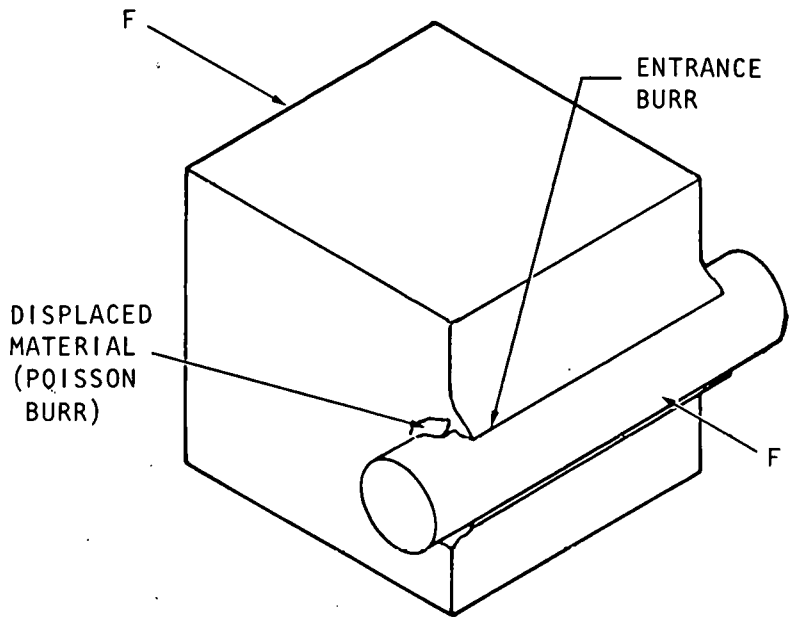

Figure 1. Formation of a Poisson Burr

p = pressure on cutting edge, and

ϕ_ρ = angle defining state of plastic flow.

Because a high pressure occurs on the tool behind the cutting edge, this model does not accurately describe the entire cutting action. If the assumption is made that the cutting force acting perpendicular to the workpiece can be treated as a concentrated line load (Figure 2), the burr thickness can be estimated from Boussinesq's formula for stresses in a semi-infinite plate subjected to line loads:

$$b_t = \frac{F_A}{C_1\sqrt{3}b\sigma_e}; \qquad (4)$$

where

F_A = the force normal to the cut surface; and

C_1 = a constant.

Although the theory developed by Boussinesq indicates that C_1 should be 0.91, empirical results indicate that it is nearly 3.0 for ductile materials.

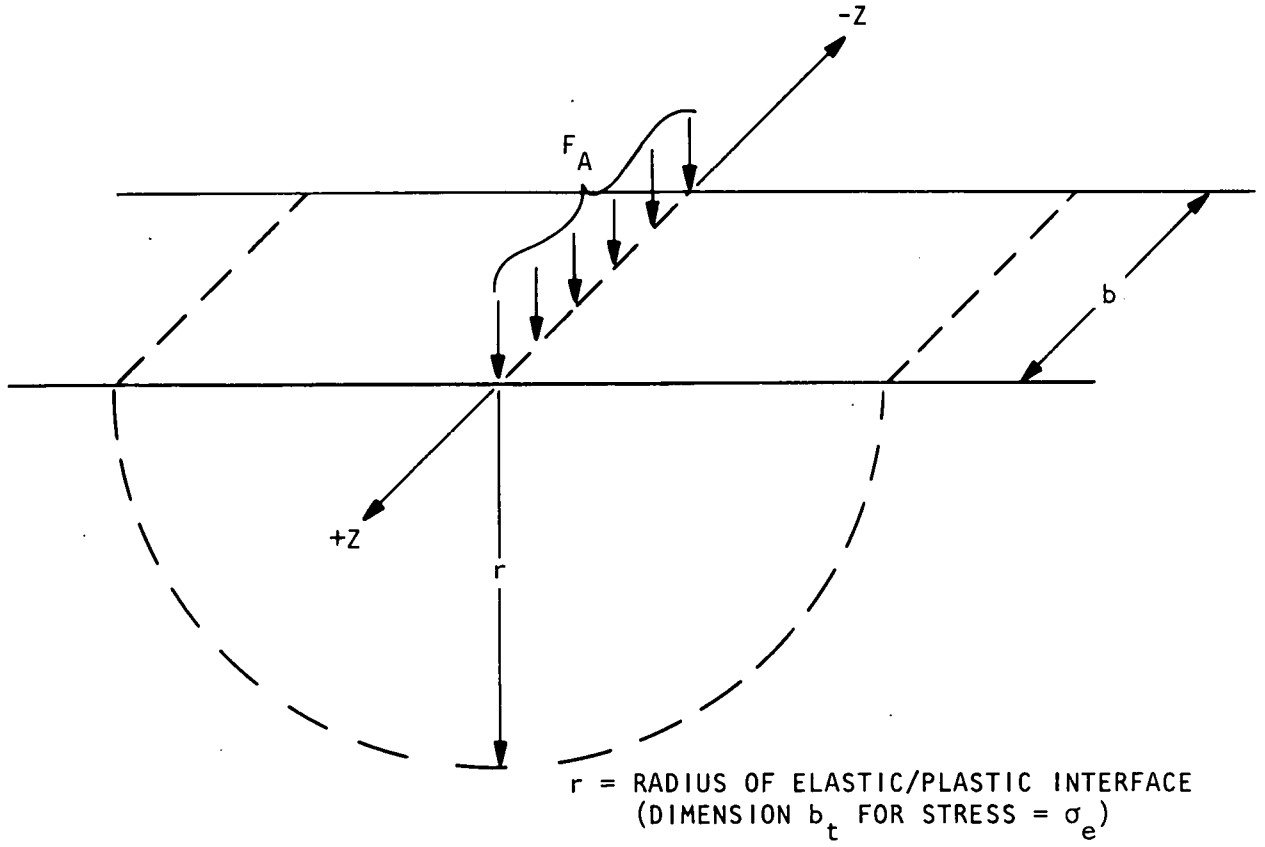

Figure 2. Line Load Applied to a Semi-Infinite Plate of Thickness b

While F_A can be easily measured, it also can be predicted for sharp tools from either of the following equations.

$$F_A = 396{,}000\ fbW_N \tan(\tau-\alpha), \tag{5}$$

or

$$F_A = fb\sigma_s \left[\tan\left(\frac{C+\tau-\alpha}{2}\right) + \text{cotan}\left(\frac{C-\tau+\alpha}{2}\right)\right]\left[\tan(\tau-\alpha)\right], \tag{6}$$

where

f = feedrate (ipr),

W_N = unit power (hp/in.^{3}/min),

σ_s = shear stress of the workpiece material,

C = a material constant,

τ = friction angle = arc tan μ,

μ = coefficient of friction between chip and tool, and

α = tool-rake angle.

Thus by knowing only the yield stress of a workpiece and some of the cutting parameters, the thickness of the Poisson burrs can be calculated. These equations indicate that any variable which increases the cutting forces in a given material will increase the burr thickness. Therefore, faster feedrates and dull tools will increase the burr thickness. Note that deeper cuts do not influence burr thickness since there is a b in both the numerator and denominator of the fraction.

Because reduced tool clearance and rake angles will increase the cutting forces, they also will increase the burr size. As indicated in Equation 2, large radii on cutting edges will increase the burr thickness.

Entrance Burr

When the cutting edge first indents the workpiece, another type of burr may be formed (Figure 3). This entrance burr consists of material which has flowed in a direction opposite that of the tool. It is similar to the ridge which forms around the indentation made by a Brinell hardness tester.

Whether or not a burr is formed at this point depends on the workpiece properties and, probably, the actual shape of the cutting edge. Assuming that the effects produced by a cylinder indenting metal are somewhat similar to those produced by a ball indenting metal, the strain-hardening of the material plays an important role. Based on Brinell hardness results, a lip of material has been shown to form whenever the material has a low strain-hardening exponent (Figures 4 and 5). In this case, the burr will be long and narrow.

Materials having a high strain-hardening exponent cause a bulge, but not a sharp burr. Assuming a constancy of volume, this bulge will be wide but short--probably so short that it is difficult to detect. Essentially, this entrance burr is one form of a Poisson burr.

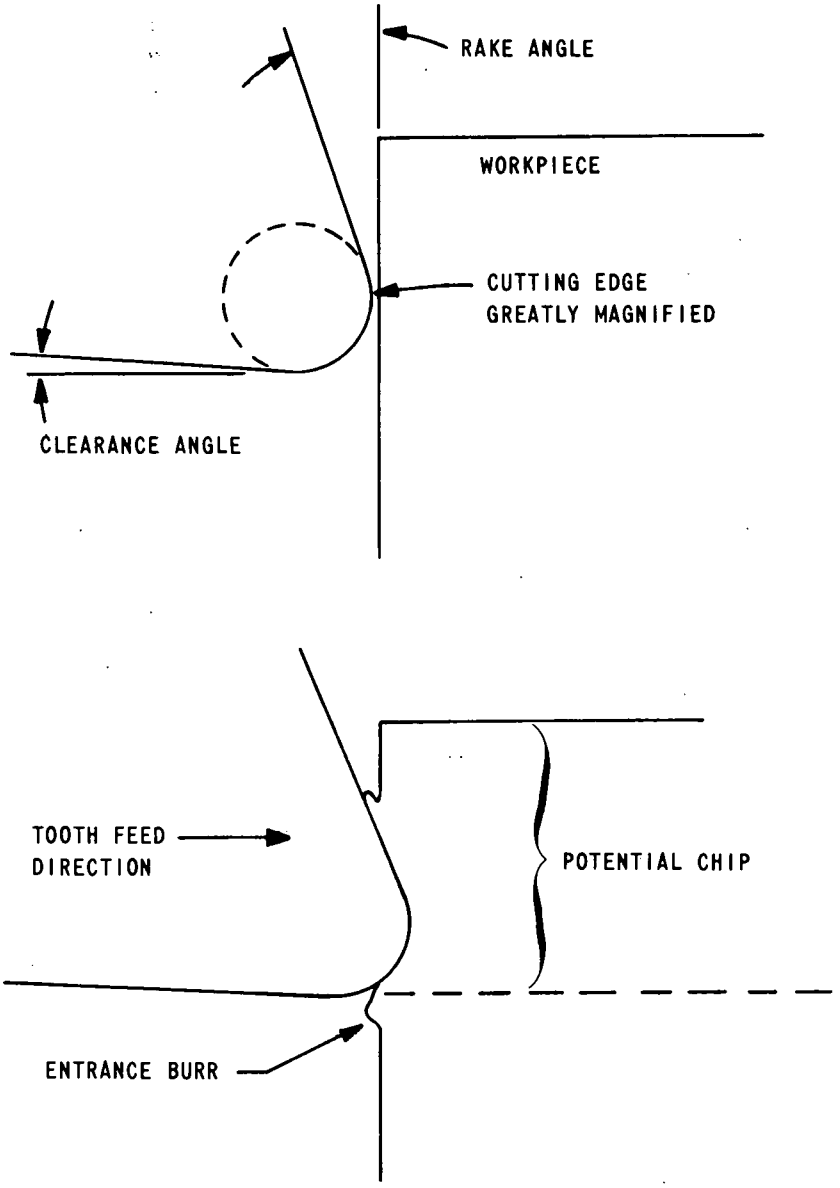

Figure 3. Cutting Edge Producing Indentation as It Enters Workpiece

Roll-Over Burrs

When a cutting edge exits from a workpiece, a roll-over burr is formed in those cases in which the chip is easier to bend than to cut (Figure 6). The thickness of this type of burr can be estimated by using Equation 7 for a perfectly plastic material, and Equation 8 for a strain-hardening material.

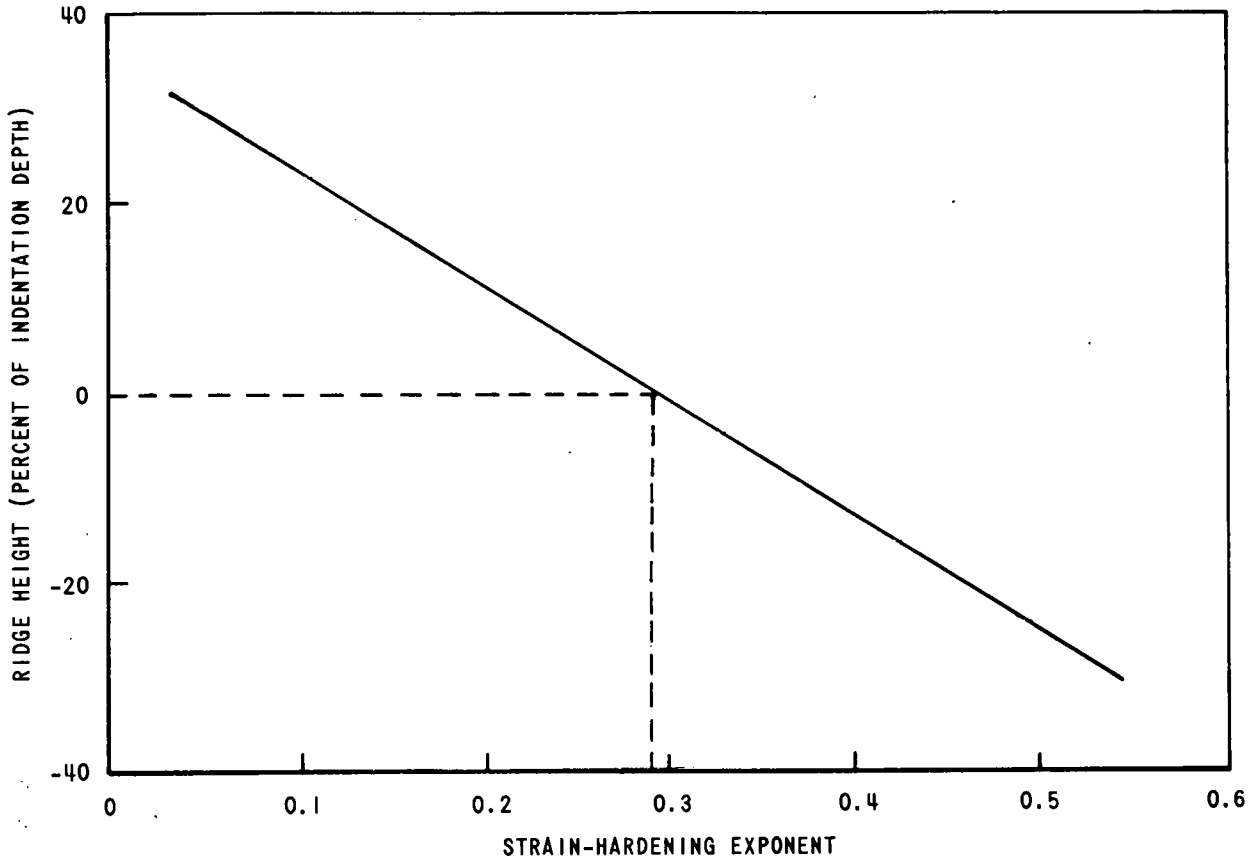

Figure 4. Effect of Strain-Hardening Exponent on Ridging-Burr Formation

Figure 5. Material Displacement, Using Spherical Indenters

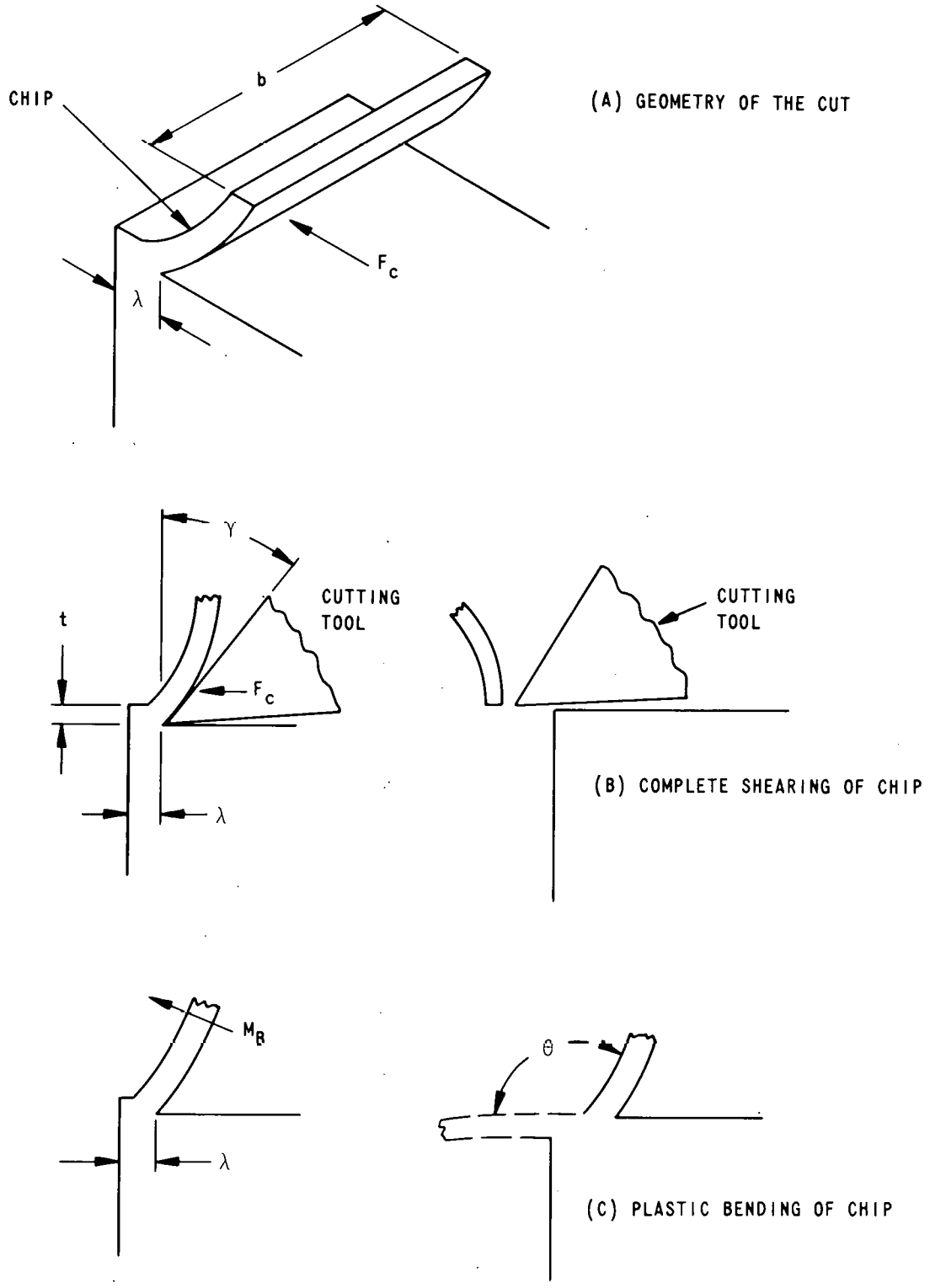

Figure 6. Chip-Deformation Modes at End of Cut

For $\lambda \leq \frac{t}{\tan \phi}$,

$$\lambda = \left(2F_c + \sqrt{4F_c^2 - \frac{C_2 2b\sigma_e \theta t F_c}{\tan \phi}}\right)\left(\frac{1}{C_2 b\sigma_e \theta}\right); \quad (7)$$

for $\lambda \geq \frac{t}{\tan \phi}$,

$$\lambda = \left[2F_c + \sqrt{4F_c^2 - \frac{C_2 2b\sigma_o \varepsilon_f^n t \theta F_c}{(n+1)\tan \phi}}\right]\left[\frac{n+1}{C_2 b\sigma_o \theta \varepsilon_f^n}\right]; \quad (8)$$

where

λ = burr thickness,

F_c = principal cutting force,

t = uncut chip thickness = feedrate (f) in turning,

ϕ = shear angle in cutting = $\frac{c-\tau+\alpha}{2}$,

θ = the angle through which the burr is bent ($\pi/2$ + rake angle), and

C_2 = a constant expressing the ratio of redundant work to theoretical work in bending.

Equation 8 is applicable when the workpiece material strain-hardens according to the following equation.

$$\sigma = \sigma_o \varepsilon^n. \quad (9)$$

Most materials can be approximated by this formula. To obtain an average value of σ_e for use in Equation 7, Equation 9 must be integrated over the total strain range. This results in an effective yield strength that is expressed by Equation 10.

$$\sigma_e = \frac{\sigma_o \varepsilon_f^n}{n+1}, \quad (10)$$

where

σ_o = material stress at a true strain of 1.0,

ε_f = true strain at fracture, and

n = strain-hardening exponent.

Note that Equation 8 is simply Equation 7 with the value of σ_e inserted from Equation 10. For most situations, the constant C_2 is in the order of 3.0. The principal cutting force F_c can be estimated from either of the following two equations.

$$F_c = 396{,}000\ bfW_N, \tag{11}$$

or

$$F_c = fb\sigma_s\left[\tan\left(\frac{c+\tau-\alpha}{2}\right) + \operatorname{cotan}\left(\frac{c-\tau+\alpha}{2}\right)\right]. \tag{12}$$

The length of a roll-over burr, which is a function of the cutting conditions and the plasticity of the workpiece, cannot be greater than the total depth-of-cut. If, in bending, the strain exceeds the strain required to fracture, most of the burr will break off and leave only a short piece attached to the workpiece.

Because hardness is a direct function of strength (and therefore also of the strain), the fact is obvious that the highly strained burrs are harder than the basic workpiece. For all practical purposes, the average hardness of the burr at its base approaches one-half the sum of the parent-material hardness and the hardness of the same material in the fully work-hardened condition.

Although it is not obvious, the burr thickness is a linear function of the depth-of-cut (t) or, in turning, of the feedrate (f). As in the case of the Poisson burr, any factor other than the depth-of-cut which increases the cutting force will increase the burr thickness.

Tear Burrs

Tear burrs are formed when the chip is torn rather than sheared from the workpiece. Although this type of burr can result from most of the basic cutting processes, its formation can be most easily visualized through side-milling operations. As shown in Figure 7, the cutter tooth forces the chip upward and forward while the sides of the chip are being torn from the workpiece. The torn portion which remains on the workpiece constitutes the tear burr. This burr can be formed by either of two mechanisms (Figure 8): the tooth can stretch the material in such a way that the burr is formed through bending, or it can shear the metal. The mechanism which predominates appears to be a function of the cutting velocity and the workpiece properties. At the present time, however, no quantitative theory exists for predicting the properties of the tear burr.

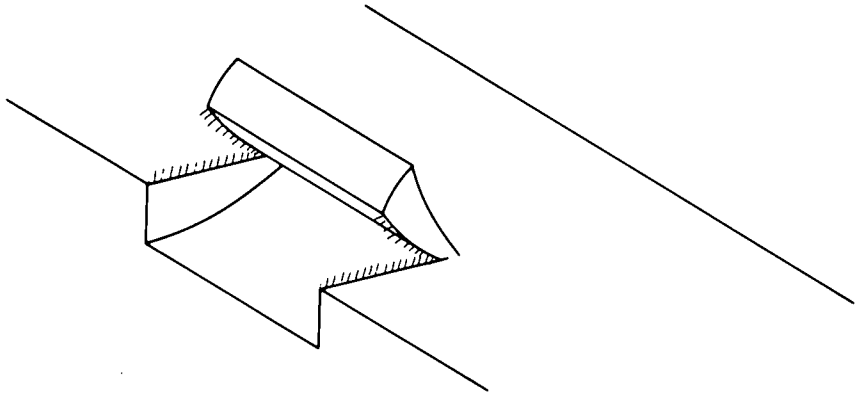

Figure 7. Separation of Initial Side-Milling Chip

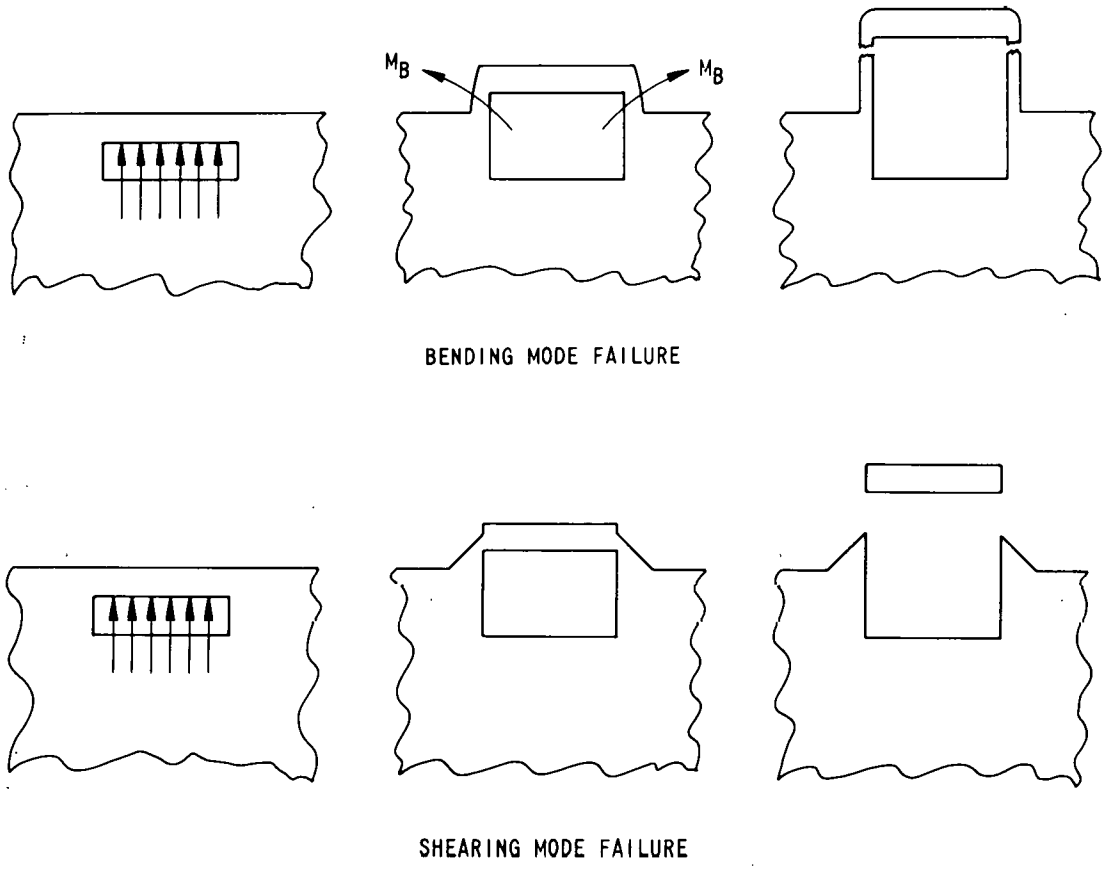

Figure 8. Tear-Burr Modes of Failure

Burr Radius

The Poisson burr, the roll-over burr, and the tear burr all have one property which has not been discussed: a radius is produced on their back side (Figure 9). The cross section of the burr can be expressed by height b_L, thickness b_t, and radius b_r. Although some individuals consider b_{min} to be the burr thickness, when all of the burr must be removed, b_t best defines its thickness. More significantly, b_{min} cannot be easily defined for some burrs (Figure 10).

For Poisson burrs, the radii are actually exponential functions. Although a theory has not been developed for b_r for a roll-over burr, some of the theory developed for sheet-metal bending appears to be applicable.

The Cutoff Projection

Whenever a part is allowed to fall from the bar stock before the cutter has cut completely through the stock, a cutoff projection is formed. As the cutoff tool nears the center of the workpiece, the high-thrust forces bend the thin cylinder of material which holds the workpiece to the stock. Shortly after bending begins, the part fractures from and falls free of the stock. The small cylinder of material which remains on the workpiece constitutes the cutoff projection.

As previously mentioned, the cutoff projection is not a true burr, since it is not produced by plastic deformation. It generally must be removed, however, and therefore it presents some of the same problems as do burrs. For this reason, it often is called a burr and is treated as such.

Burrs Produced by Specific Turning Operations

In an operation which involves only turning, a Poisson burr forms on the outside diameter of the part (Figure 11). In a grooving or cutoff operation, a tear burr forms at the sides of the groove (Figures 11 and 12). If the tool rubs the sides of the groove because of too little clearance, the burrs become larger as the result of additional plastic flow. If the turning tool passes over a groove or an axial slot in the workpiece, a roll-over burr is formed (Figure 13).

In a face-and-turn operation (Figure 14), a roll-over burr is formed on the outer diameter of the part. Note however that if the tool were fed inward rather than outward, a tear burr would be produced. The cutoff projection occurs when a parting or cutoff tool separates the part from the bar stock (Figure 15).

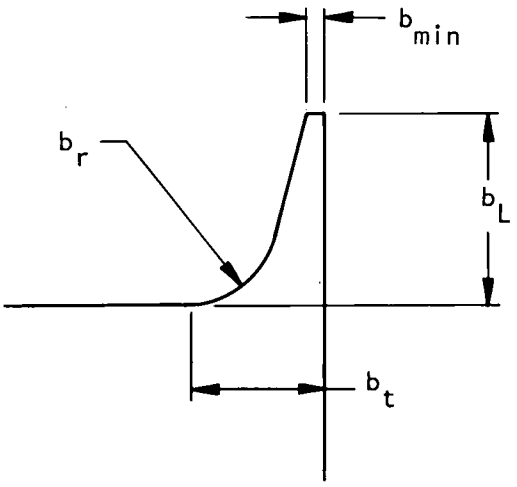

Figure 9. Cross Section of Typical Machining Burr

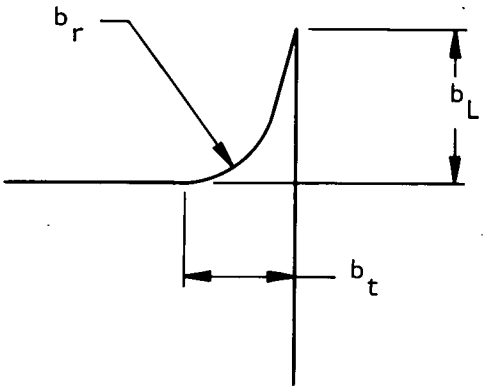

Figure 10. Cross Section of Typical Blanking and Some Machining Burrs

Because metal-cutting involves plastic deformation of the material, burrs cannot be prevented by adjusting the cutting parameters. They can be minimized, however, and some of the burrs can be prevented by controlling the part shape where certain geometries are involved.

Test Results

Two studies were performed to determine how turning parameters affect burr size. In the first study, the radial depth-of-cut,

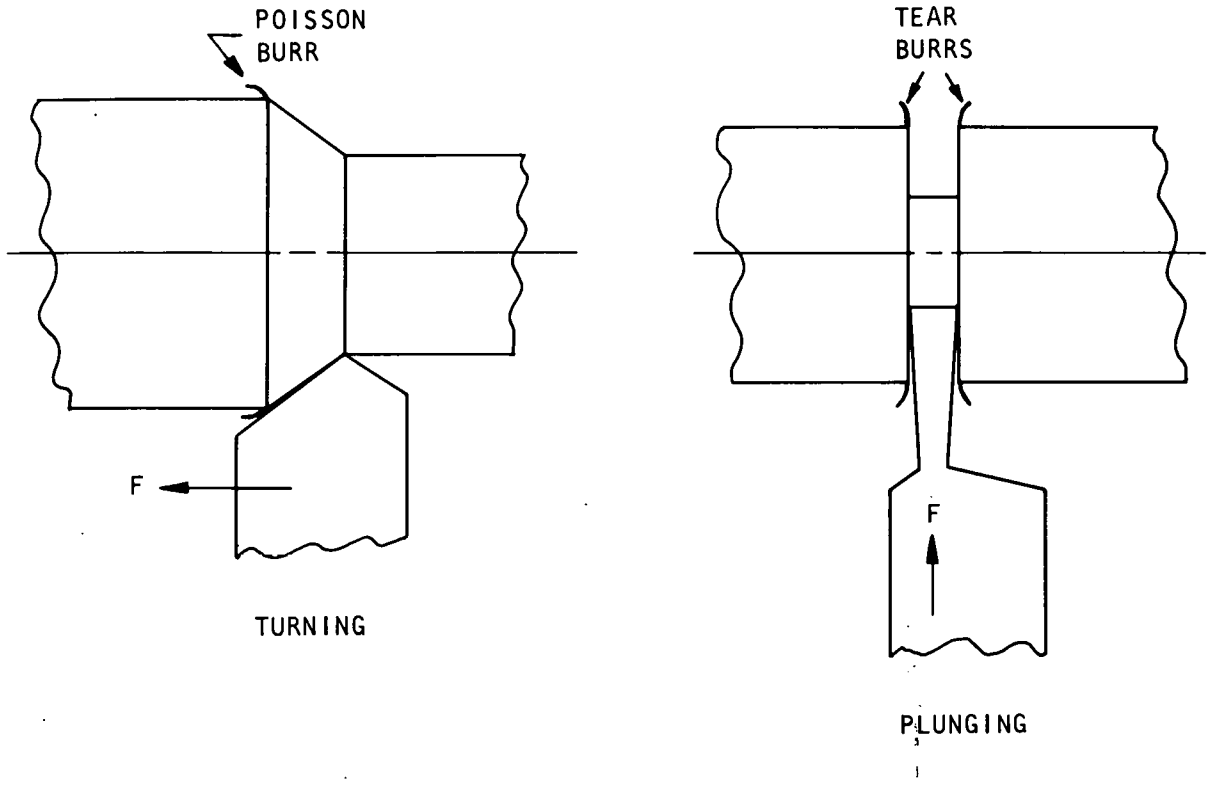

Figure 11. Burrs Formed in the Basic Turning Operations

feedrate, rake angle, and side-cutting edge angle (SCEA) were varied. The workpiece material consisted of 303Se stainless steel. In the second study, the end-cutting edge angle (ECEA), end relief, back rake, side rake, SCEA, and radial depth-of-cut were studied in five materials. A brief study of burrs that are typically produced in the manufacture of parts also was performed.

Test 1: Effect of Turning Variables in 303Se Stainless Steel

To determine the effects of the SCEA, radial depth-of-cut, feedrate, and rake angle on Poisson turning burrs, 53 specimens were machined and measured. The workpiece material consisted of 12.7-mm-diameter (0.5 inch) 303Se stainless steel in the cold-drawn condition (R_C28). Table 1 shows the ranges of the variables that were studied, and Appendix Table A-1 lists the parameters and results for each specimen. Carbide-insert cutting tools were used for all cuts. With the exception of the rake angles, all variables were tried at all combinations shown.

A negative SCEA was employed in both this and the second test. A negative-SCEA cutting tool is defined as a tool in which the nose radius leads the cutting edge (Figure 16). This type of

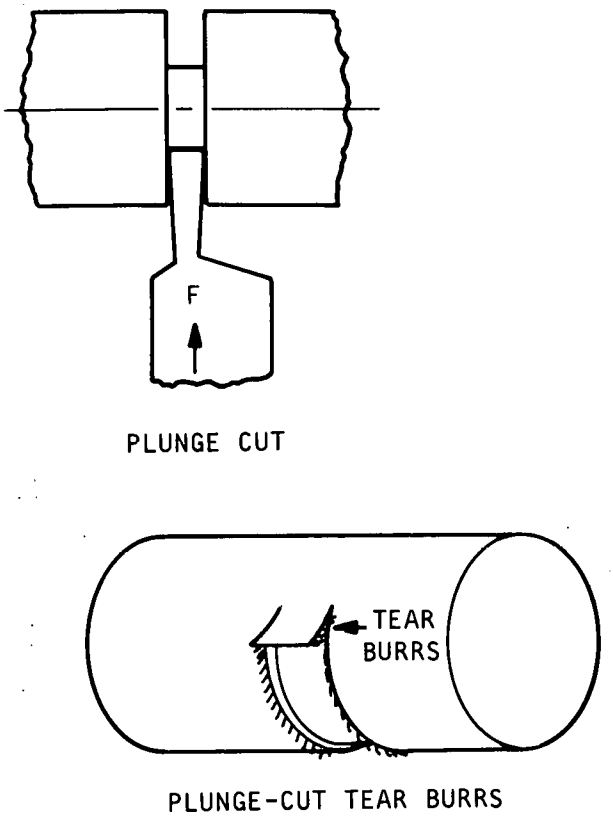

Figure 12. Formation of Tear Burrs

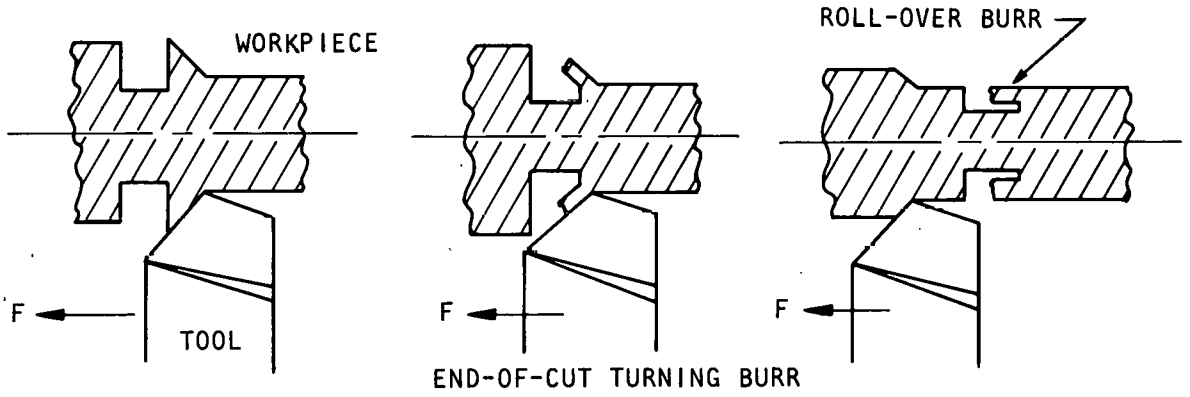

Figure 13. Roll-Over Burr Produced by Turning

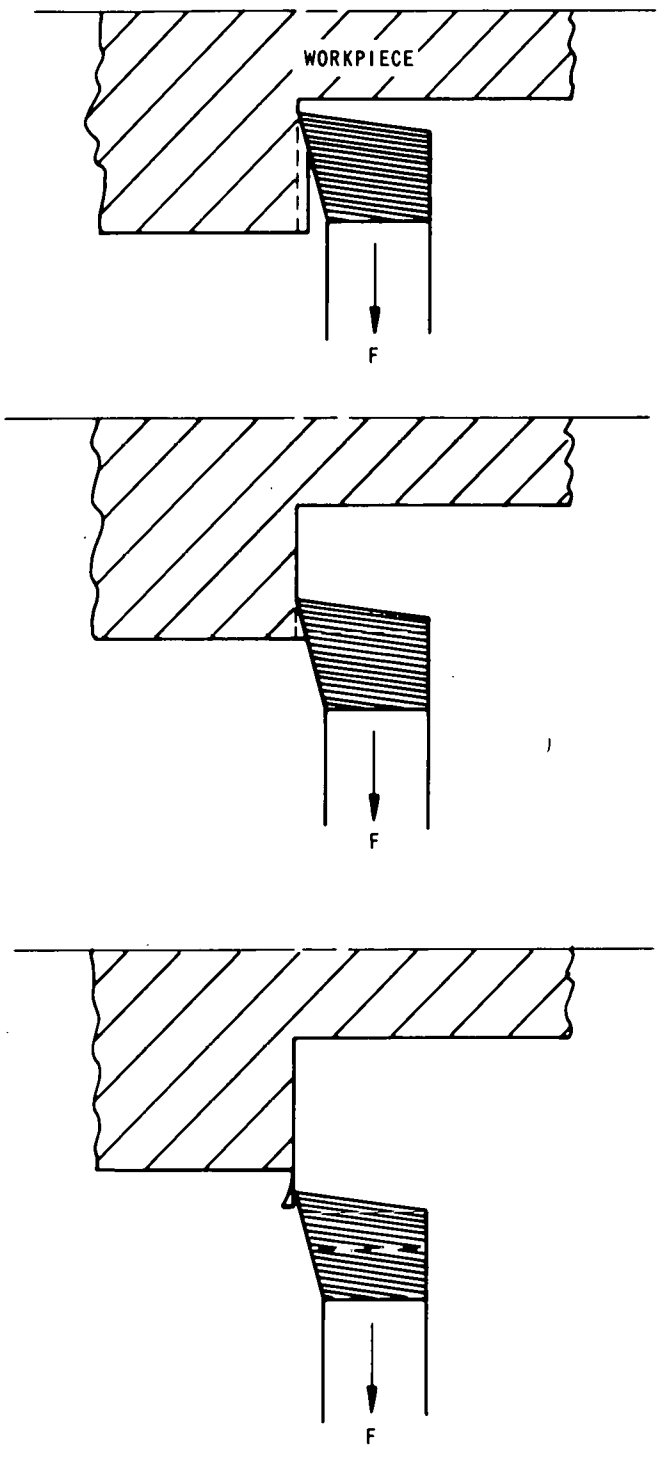

Figure 14. Roll-Over Burr Produced by Facing

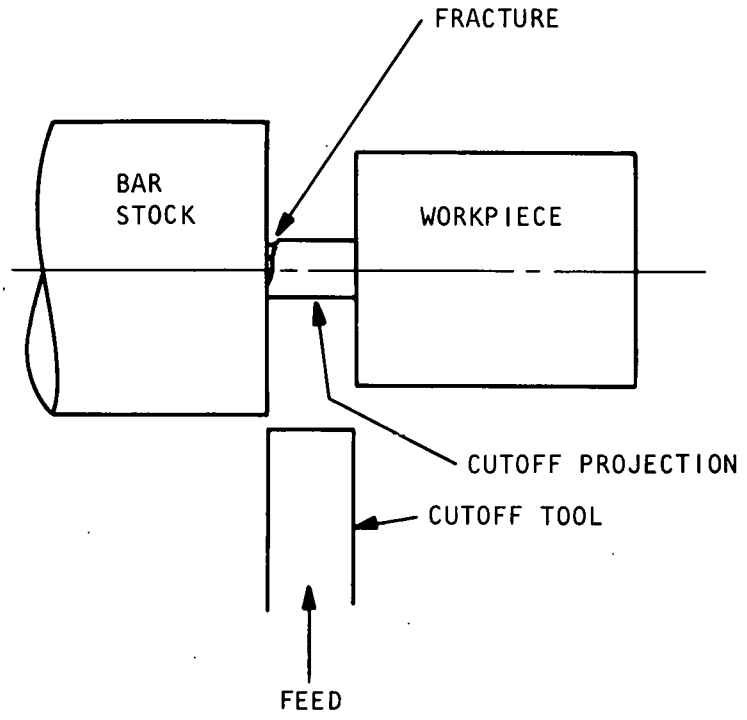

Figure 15. Formation of Cutoff Projection

tool is required for a turn-and-face operation to produce a perpendicular shoulder on the part (Figure 14). While a tool having an SCEA of zero also can produce a shoulder, it frequently will result in chatter marks on the part.

The SCEA, depth-of-cut, and feedrate all significantly affected the height of the burrs that were produced. All interactions between these variables also were of significance. As shown in Appendix Table A-1, the impact of these variables was obvious even without computer analysis.

The tremendous influence of SCEA on the burr height and thickness appears to be the result of a built-up edge (BUE) on the cutting edge of the tool and high strain-hardening of the workpiece. Negative SCEAs are frequently used in precision finishing operations, but the burr sizes do not approach those that were observed in this study. The following three factors appear to be responsible for this anomaly.

- Workpiece vibration allowed the tool to rub the workpiece before entering the cut.
- A built-up edge occured when SCEAs of 0 and -17-1/2 degrees were used, and this BUE generated forces similar to those produced by a dull tool.

Table 1. Variables Studied in Turning Tests

SCEA (Degrees)	Depth-of-Cut (mm; Inch)	Feedrate (μm/Revolution; IPR)	Rake Angle (Degrees)
17-1/2	1.016 (0.040)	53.3 (0.0021)	15
0	1.778 (0.070)	81.3 (0.0032)	5
-17-1/2	2.540 (0.100)	109.2 (0.0043)	-4.3
		165.1 (0.0065)	

- The chip-breaker groove was filled by BUE material at SCEAs of 0 and -17-1/2 degrees, thus preventing adequate chip flow.

Essentially, the slenderness of the workpiece appeared to allow the cutting tool to skip in and out of the cut and consequently produce a great amount of rubbing which work-hardened the surface and increased the cutting difficulty. Rather than being sheared as in normal cutting, the material at the edge flowed outward laterally and formed a burr. The fact that no coolant was used and that the tool kept the chip near the workpiece rather than moving it away from the workpiece accentuated the problem. In some instances, red-hot chips were produced. Under this situation, the material became very gummy and further restricted the cutting. As material became welded in the chip-breaker groove, it effectively produced a negative-rake tool which restricted the flow even more.

The described conditions apparently could be prevented by using a flood coolant and feedrates that are better matched to the workpiece stiffness. Eliminating the chip-breaker groove also should help to produce easier cutting.

For this particular study, the tool was not fed outward radially as normally would be done in a production situation. This allowed the true shape of the Poisson burr to be observed. Facing outward would have resulted in a roll-over rather than a Poisson burr (Figure 17).

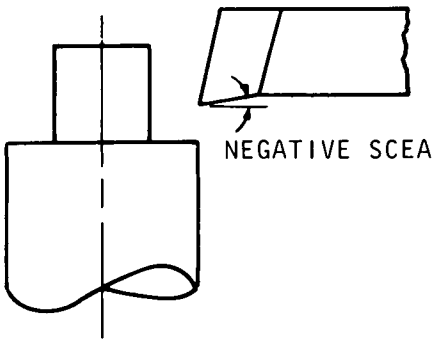

CONVENTIONAL TURNING TOOL

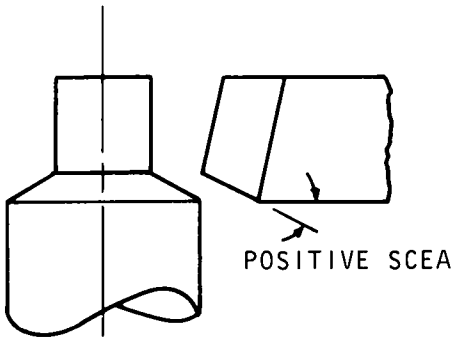

FACE-AND-TURN TOOL

Figure 16. Comparison Between Face-And-Turn and Conventional Turning Tools

The assumptions that were made in deriving the Poisson burr equations appear to be satisfied by the data presented in Figures 18 through 20. An increase in the feedrate caused a slight increase in the burr size. If ϕ_a in Equation 1 were -60 degrees, the predicted burr thickness in this material would be 0.4 times the effective cutting radius. A cemented carbide tool could easily have a cutting-edge radius of 50.8 μm (0.0020 inch) which would predict a 20.3-μm-thick (0.0008 inch) burr. As noted in Figure 18, a typical burr thickness would be 25.4 μm (0.0010 inch).

In this test, the height of the Poisson burrs was only slightly affected by the feedrate (Figure 19). As shown in Figure 20, the burr height was proportional to the depth-of-cut. This agrees with the theory (Equation 3). Again assuming that

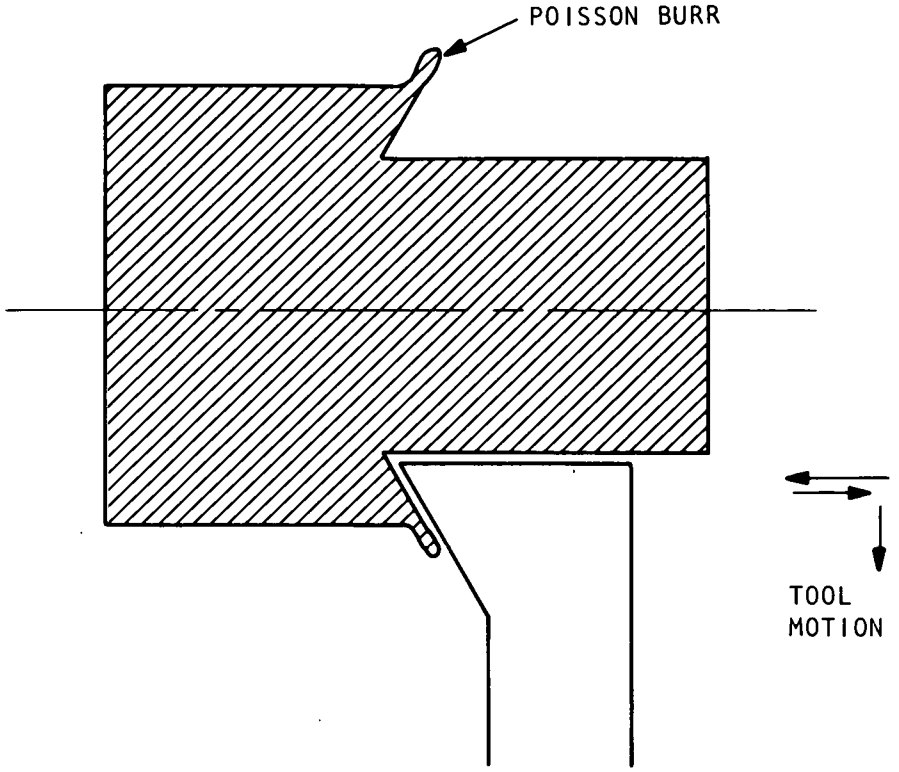

Figure 17. Tool Motion Utilized to Leave Undisturbed the Poisson Burr Produced by the Negative-SCEA Tool

ϕ_a = -60 degrees and that ν = 0.3, E = 206,820 MPa (30 x 10^6 psi), and σ_e (the yield stress of an equivalent perfectly plastic material) = 1103 MPa (160,000 psi), the burr height is predicted by the following equation.

$$b_L \simeq \frac{b}{2}\left(-\frac{\sin\phi}{\sqrt{3}\cos\phi + \sin\phi}\right) \qquad (13)$$

When ϕ is a small negative angle (from 0 to -30 degrees, for example), b_L ranges from 0 to b/1.4. Thus, provided that ϕ is a small negative angle, the height predictions are in the correct order of magnitude.

In most turning operations, the tool is allowed to dwell at a shoulder before it is retracted. Although this procedure is necessary to produce an even shoulder, the fact that this dwell could influence the size of the burr is not difficult to envision.

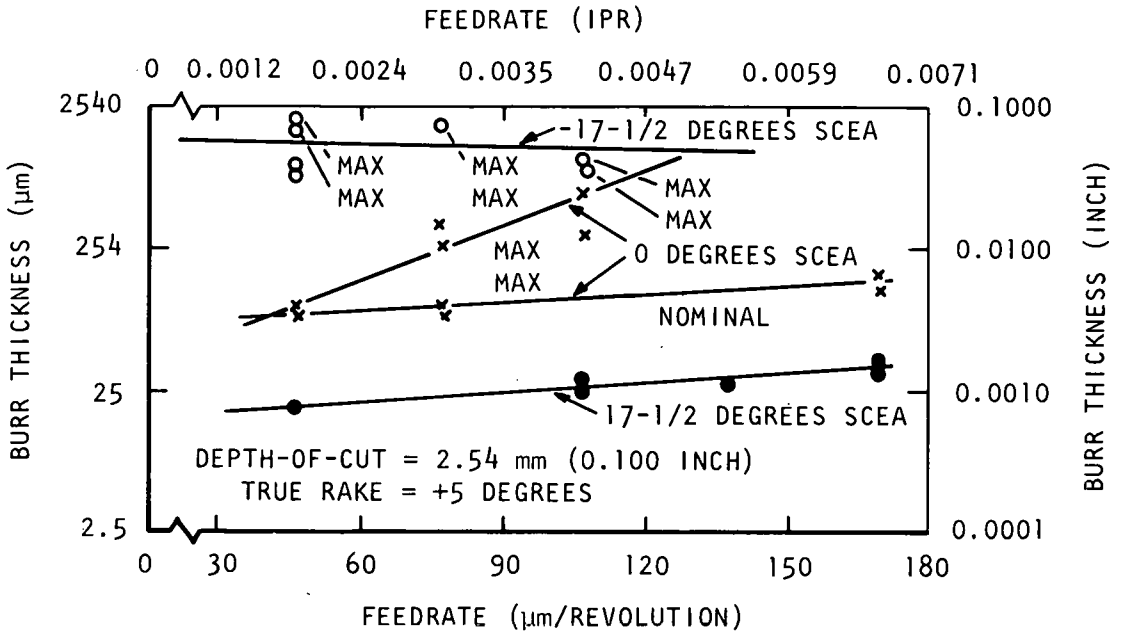

Figure 18. Effect of Feedrate and SCEA on Poisson-Burr Thickness in a Turning Operation

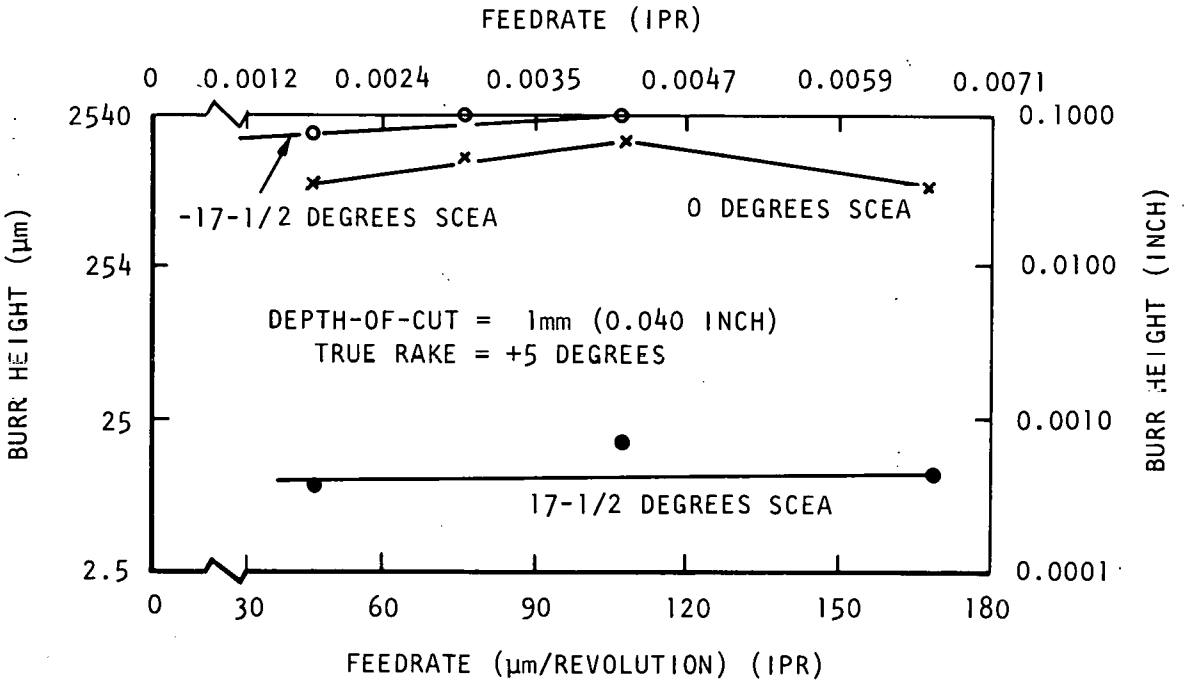

Figure 19. Effect of Feedrate and SCEA on Poisson-Burr Height in a Turning Operation

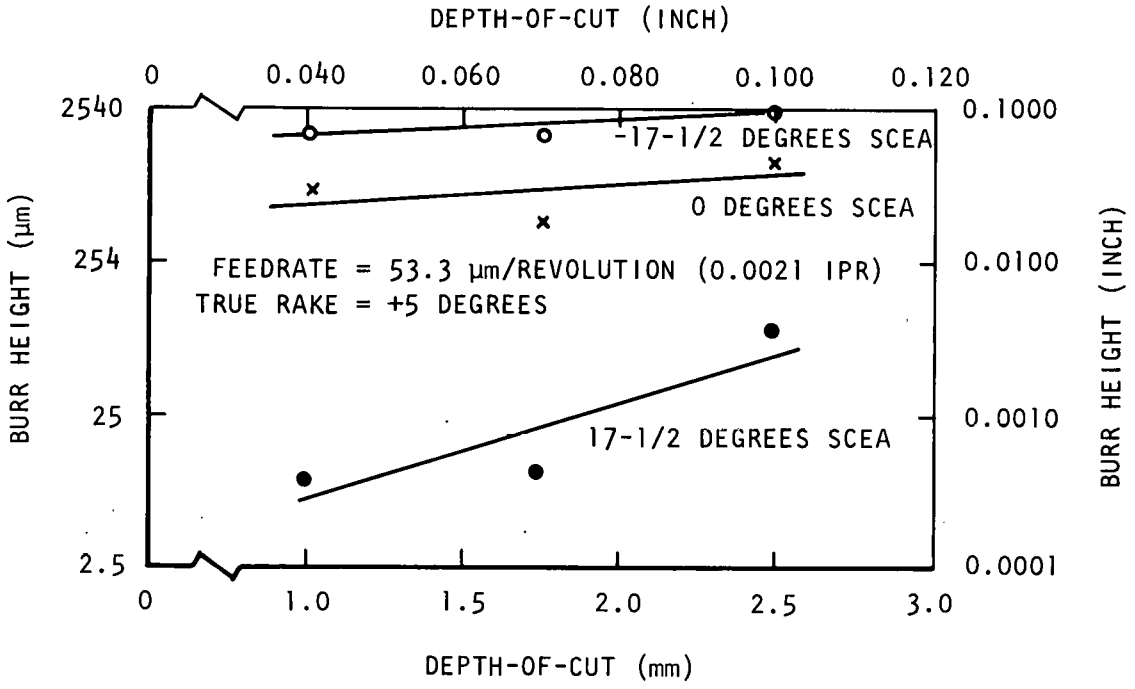

Figure 20. Effect of Depth-Of-Cut and SCEA on Poisson-Burr Height in a Turning Operation

The influence could be the result of either rubbing or the fact that the tool is making a clean-up cut during the first revolution of the workpiece after the feed has been stopped. This clean-up cut varies in thickness from zero to whatever the feed had been per revolution. For materials that are feedrate-sensitive, this could produce a burr which varies around the diameter of the part. This effect has been noted with some materials.

In these tests and in other work with 304 stainless steel and 1020 cold-rolled steel, the height of the very large burrs has been observed to be proportional to the axial length-of-cut. Apparently, this is due to the fact that the material can be pushed outward from the sides of the workpiece easier than it can be sheared. To maintain the conservation of mass, if the tool continues to advance and the material does not shear, the material must squirt out the side. This effect is similar to squeezing a tube of toothpaste: the more the tube is compressed, the longer becomes the ribbon of toothpaste.

The burr eventually is forced out radially far enough that the tangential stresses on the burr create radial cracks. The resulting burr around the workpiece then looks like the petals of a daisy, as shown in Figure 21. This burr was 0.22 mm thick

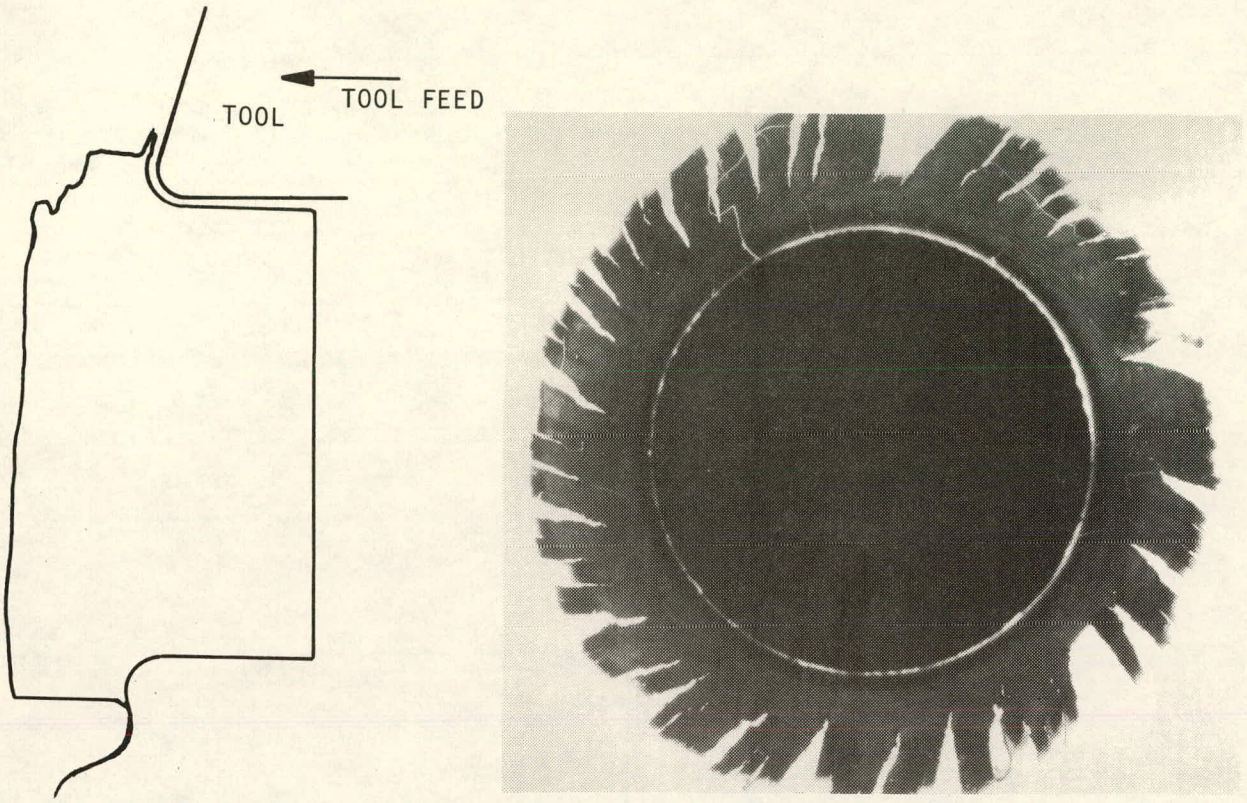

Figure 21. Illustration Showing Cutting of 303Se Stainless Steel (Left) Which Produced Poisson Burr (Right) Similar to That Illustrated in Figure 17

and 4.33 mm high (0.0088 by 0.110 inch). Its exceptional height was caused by the 0-degree SCEA of the tool.

In some cases, the radial cracking begins earlier, and the burr looks similar to numerous pieces of yarn projecting from the workpiece (Figure 22). This dependancy of the burr characteristics on the axial length-of-cut does not occur with what is considered a normal Poisson burr, the cross section of which is illustrated in Figure 23. This burr is formed by a cold-flow of the metal ahead of the tool. In precision machining using a feedrate from 20.3 to 25.4 μm/revolution (0.0008 to 0.001 ipr), a typical burr will be from 25.4 to 75.6 μm (0.001 to 0.003 inch) in both height and thickness.

Figure 24 illustrates an abnormally thick Poisson burr. A gross cold-flowing of the metal produced a height of 2.50 mm (0.100 inch) and a thickness of 0.89 mm (0.035 inch). The extreme thickness was caused by the -17-1/2-degree SCEA of the tool, which means

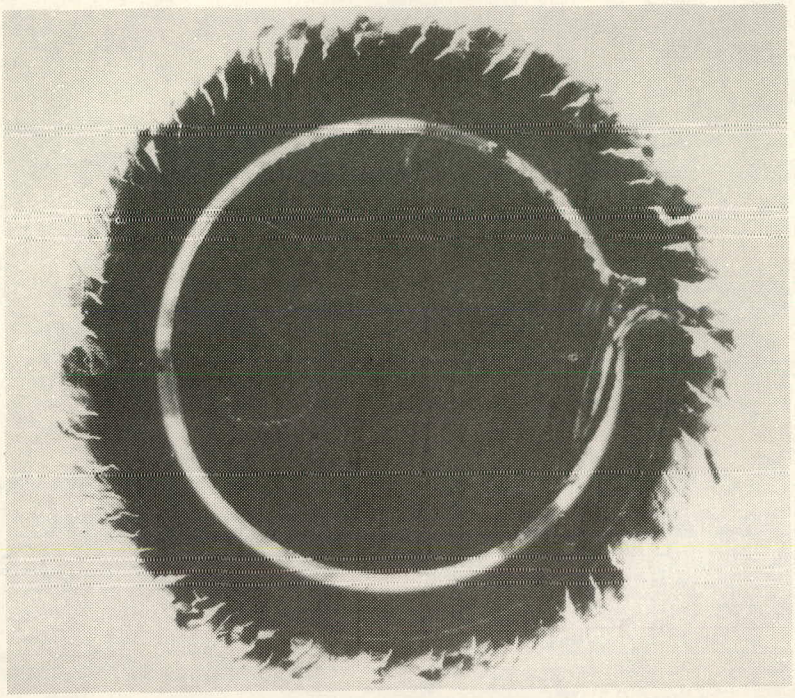

Figure 22. Poisson Burr Showing Early Radial Cracking

that the nose of the tool entered the cut before the side-cutting edge. This is not a normal machining condition.

Rake-angle effects were studied in one brief test. As shown in Figures 25 and 26, little difference was produced by the +5- and -15-degree rake angles. The -4.3-degree rake angle, which was obtained by turning the carbide insert upside down in its holder, produced burrs that were three times larger than those produced by positive rakes. With a +17-1/2-degree SCEA, the burr produced by the negative-rake tool was 50.8 μm (0.002 inch) thick, as compared with a thickness of 30.5 μm (0.0012 inch) produced by the +15-degree-rake tool. Negative rake angles appear to produce thicker and longer burrs.

A brief test of roll-over burrs formed in turning (Figures 27 and 28) indicated that a 0-degree SCEA produced thicker burrs than did a 17-1/2-degree SCEA. The effect of the depth-of-cut on this type of burr appeared to be unusually great. Because the data shown are based on only seven specimens, the results can be treated only as preliminary trends.

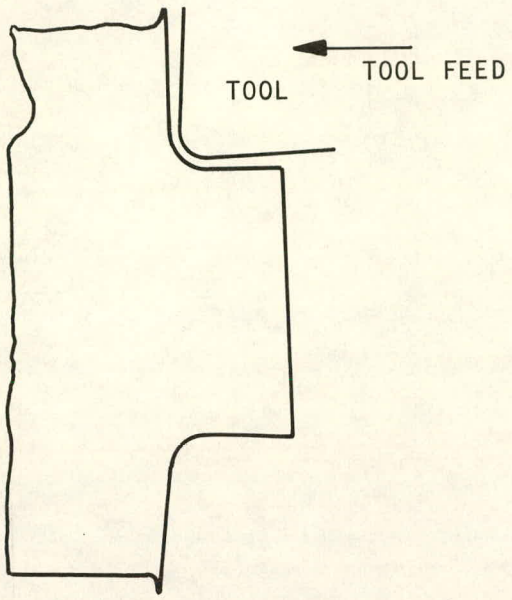

Figure 23. Illustration Showing the Formation of a Typical Poisson Burr in 303Se Stainless Steel

When the tool attempted to bend the material over into the undercut shown in Figure 13, most of the material broke free before it had been completely bent over. The result was a short burr on the workpiece and a loose ring of material encircling the workpiece.

While the hardness of the bar used in this study was typically Knoop 295 (R_C28), the burrs varied in hardness from Knoop 304 to 406 (R_C29 to R_C40). Most of the measurements indicated a typical burr hardness of Knoop 340 (R_C34).

Test 2: Effect of Workpiece Material and Tool Geometry

In the second study, five workpiece materials that are commonly used for miniature precision parts were tested. Two levels each of different tool angles were studied in combination with the radial depth-of-cut (Table 2) in a fractional factorial experiment.

All tests were performed on a super precision tool room lathe at a constant feedrate of 36.6 μm/revolution (0.00144 ipr) and a constant spindle speed of 300 rpm. The tool material consisted of M33 Cobalt high speed steel.

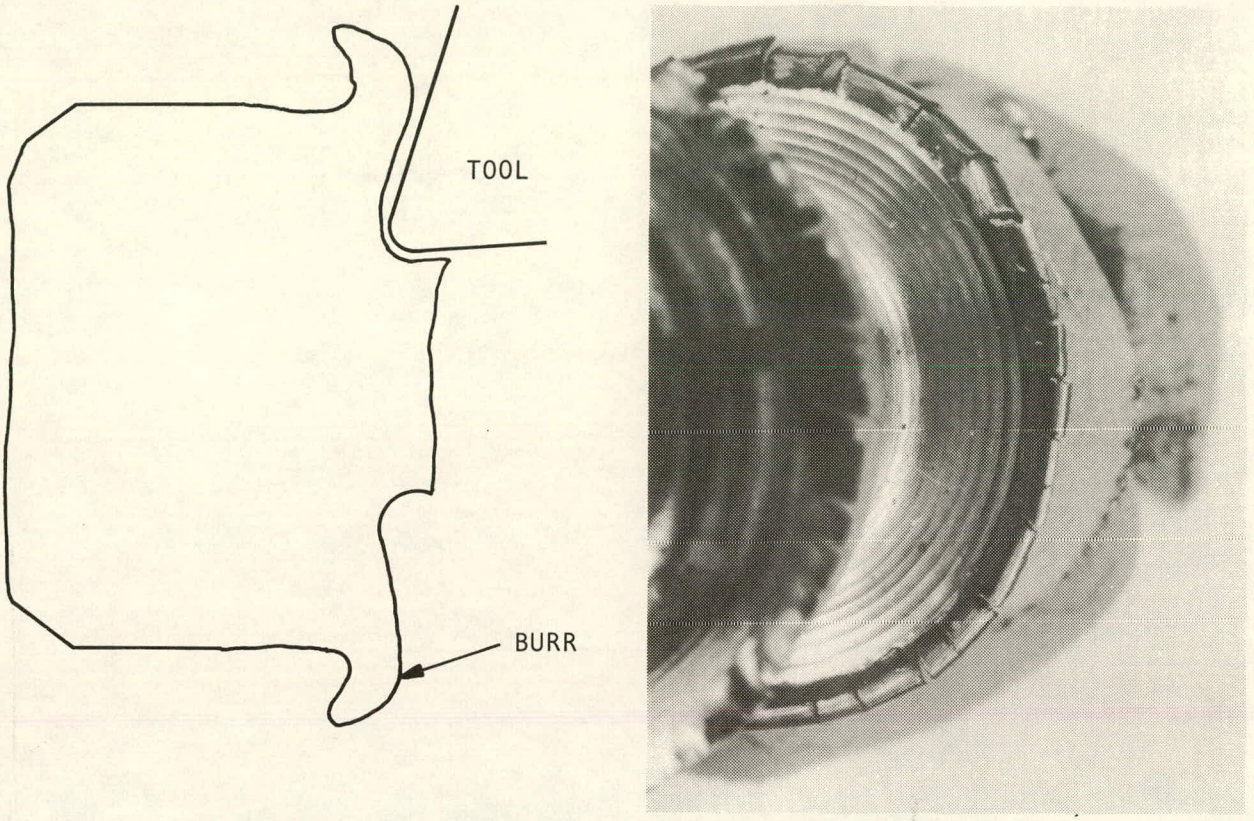

Figure 24. Illustration Showing Cutting of 303Se Stainless Steel (Left) Which Produced Abnormally Thick Poisson Burr (Right)

Cutting forces and burr size were monitored in this test, and analysis-of-variance (ANOVA) techniques were used to determine whether they were influenced by the independent test variables. Ten specimens of each material produced by each of eight tool geometries were measured. The Poisson burrs were produced in the same manner as they had been in the first test. A total of more than 2000 measurements were made in this test.

Test specimens were centerless-ground to a diameter of 24.89 mm (0.980 inch) to remove contaminating materials in the skin. Ten specimens, each 28.58 mm (1.125 inches) long, were turned with each tool. After turning to the 28.58-mm length, the tool was returned to the beginning of the cut, reset to give the desired depth-of-cut, and fed for 25.4 mm (1.0 inch). This was repeated for a total of nine passes, with each pass being 3.18 mm (0.125 inch) shorter than the previous one. This technique provided 142.875 mm (5.625 inches) of cut in a specimen only 28.575 mm (1.125 inches) long. A water-soluble coolant was used on all cuts.

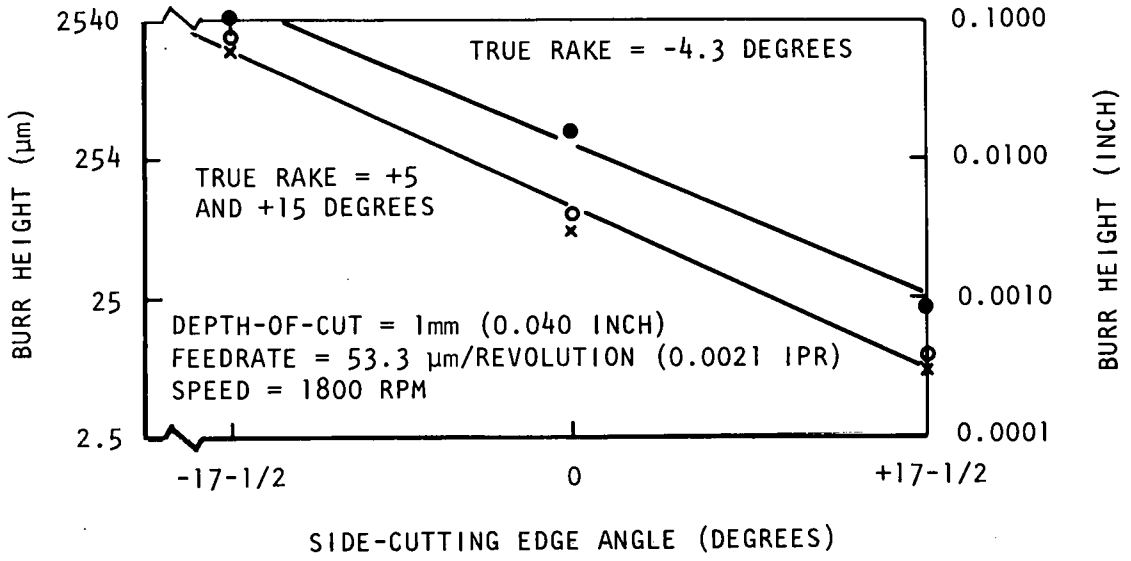

Figure 25. Effect of SCEA and True Rake on Poisson-Burr Height in a Turning Operation

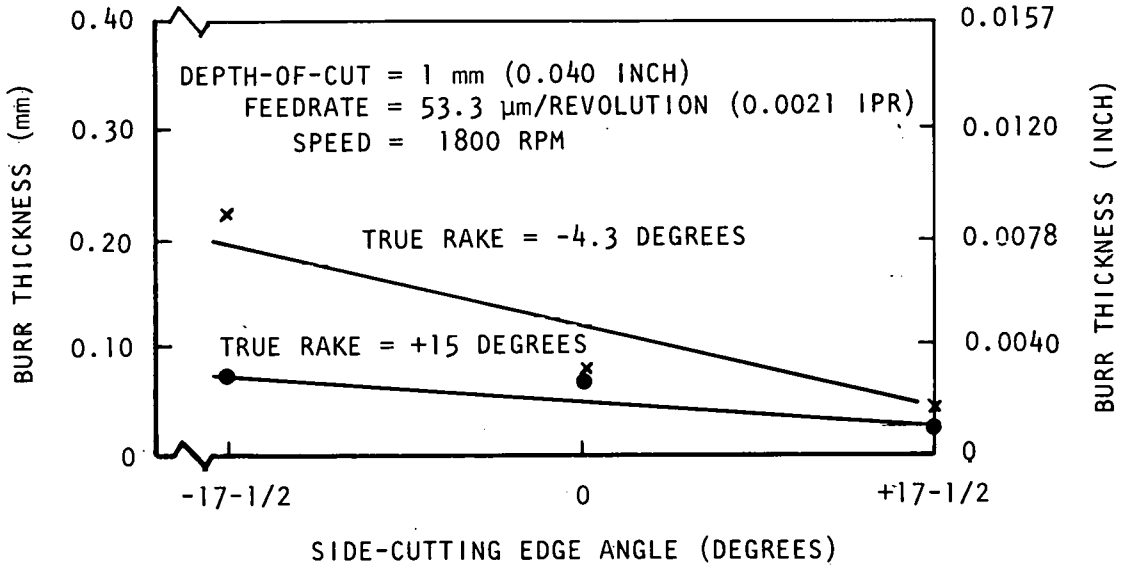

Figure 26. Effect of SCEA and True Rake on Poisson-Burr Thickness in a Turning Operation

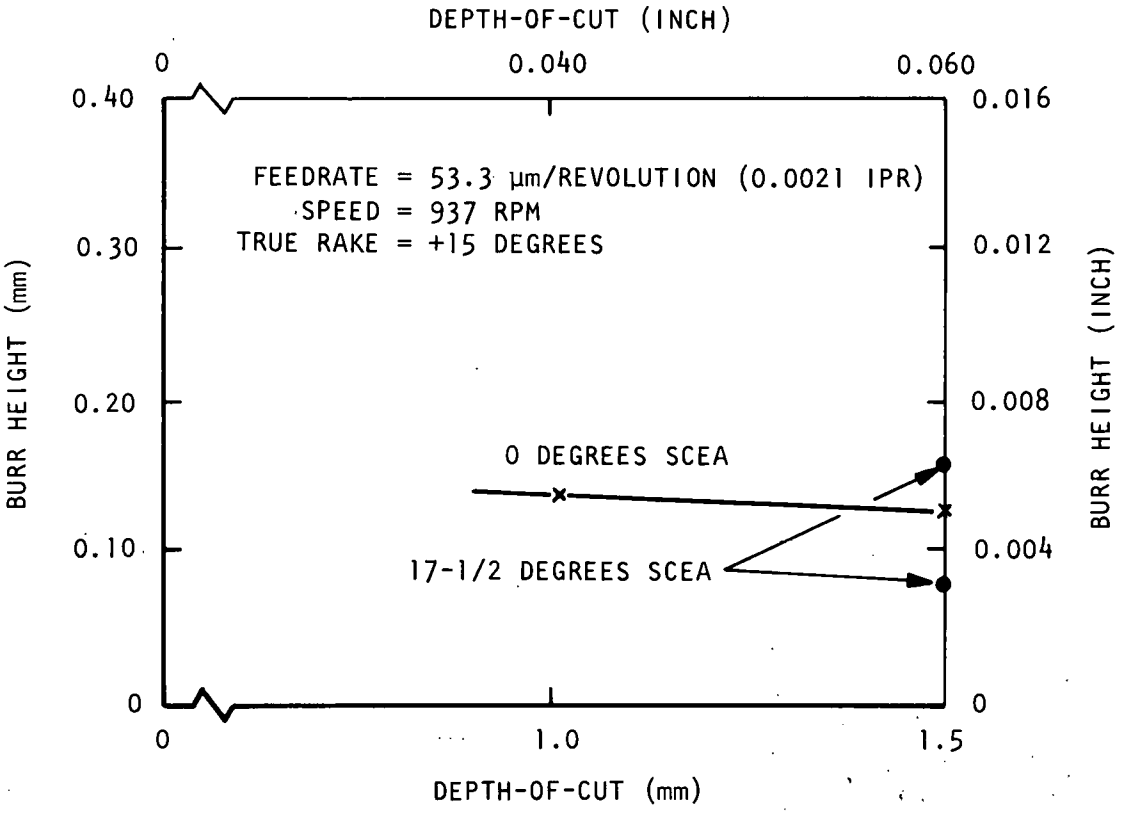

Figure 27. Effect of Depth-Of-Cut and SCEA on Roll-Over-Burr Height in a Turning Operation

Table 3 presents a composite overview of the average results that were obtained for each material. In each case, the value shown is an average from the ten specimens produced by a single tool. Definitions of the cutting forces are given in Figure 29. W_N is the calculated value of unit power for lathe operations. It is derived from the following equation:

$$W_N = \frac{HP}{12dfV} = \frac{F_T}{396{,}000\ df}; \qquad (14)$$

where

F_T = the principal cutting force (in pounds);

d = the radial depth-of-cut (in inches);

f = the feedrate (ipr); and

V = the surface velocity (sfpm).

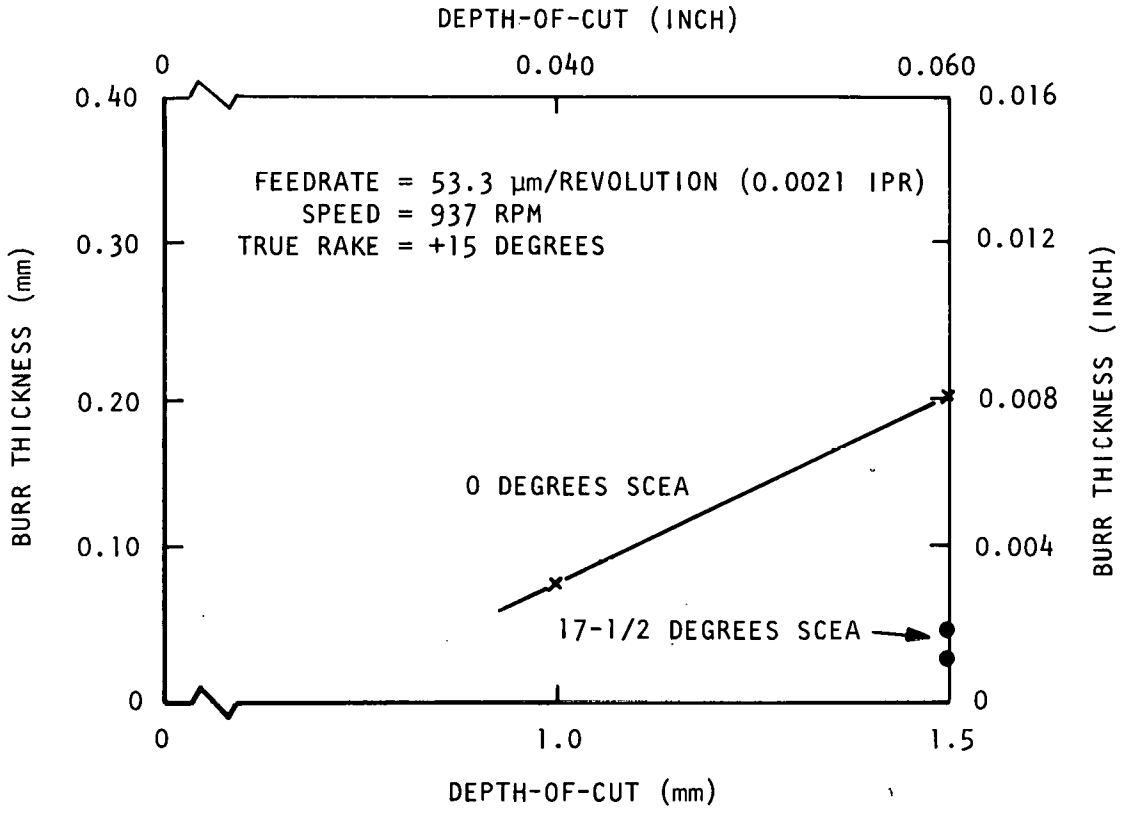

Figure 28. Effect of Depth-Of-Cut and SCEA on Roll-Over-Burr Thickness in a Turning Operation

The values of W_N that were calculated for this study are considerably larger than the typical values that are given in handbooks (Table 4). This is a direct result of using low feedrates. While W_N is relatively independent of feedrates greater than 127 µm/revolution (0.005 ipr), it is notably affected at feedrates below this value. Figure 30 illustrates the trend in 1020 steel. When handbook values of W_N are used to calculate cutting force at low feedrates, the results will be considerably less than the measured forces.

Specific Geometry Effects

The analyses of variance for burr height and thickness are shown in Tables 5 and 6. The letters in parentheses are a code for the variable. The letters in brackets indicate the interactions that were used to obtain an estimate of the variable's significance. Because this was a fractional-factorial-design test, the effect of each variable is actually confounded with higher-order interactions, as shown in Table A-2 of the Appendix. The ten

Table 2. Levels of Factors Used in Experiment

Variable and Symbol	Level 1*	Level 2	Level 3	Level 4	Level 5
A End-Cutting Edge Angle (ECEA)	7.0	2.0			
B End Relief (ERf)	10.0	5.0			
C Back Rake (BR)	5.0	0.0			
D Side Rake (SR)	10.0	5.0			
E Side-Cutting Edge Angle (SCEA)	-8.0	-2.0			
F Depth-Of-Cut	635** (0.025)	127 (0.005)			
Material	303Se	15-5PH	BeCu	Type A***	Type B****

*All "Level" values are in degrees unless otherwise noted.
**Basic "Depth-Of-Cut" values are in micrometers; parenthetical values are in inches.
***Glass sealing alloy, 53Fe-29Ni-17Co, SAE unified number K94610.
****2V permendur high magnetic permeability steel, 49Fe-49Co-2V, SAE unified number K95100.

Table 3. Typical Machining Results Produced in Various Materials

Variable Measured	Value Obtained for Material Indicated*				
	303Se	15-5PH	BeCu	Type A***	Type B****
Burr Thickness (μm; Inch)	114.3 (0.0045)	43.2 (0.0017)	55.9 (0.0022)	91.4 (0.0036)	40.6 (0.0016)
Burr Height (μm; Inch)	492.8 (0.0194)	45.7 (0.0018)	40.6 (0.0016)	208.3 (0.0082)	30.5 (0.0012)
F_T (N; Pounds)	177 (39.9)	105 (23.5)	53 (12.0)	86 (19.4)	180 (40.4)
F_A (N; Pounds)	97 (21.9)	52 (11.7)	21 (4.7)	43 (9.7)	82 (18.4)
F_R (N; Pounds)	33 (7.5)	4 (1.0)	5 (1.1)	3 (0.7)	45 (10.1)
W_N** ($W/cm^3/s$; $HP/in.^3/min$)	3.57 (4.7)	2.35 (3.1)	1.29 (1.7)	1.75 (2.3)	3.80 (5.0)

*Value shown is the average for eight tool-geometry/depth-of-cut combinations; each tool produced ten specimens each 142.9 mm (5.625 inches) long; one reading was taken on each specimen.

**W_N is the calculated value for unit power; averages shown exclude unusually large values.

***Glass sealing alloy, 53Fe-29Ni-17Co, SAE unified number K94610.

****2V permendur high magnetic permeability steel, 49Fe-49Co-2V, SAE unified number K95100.

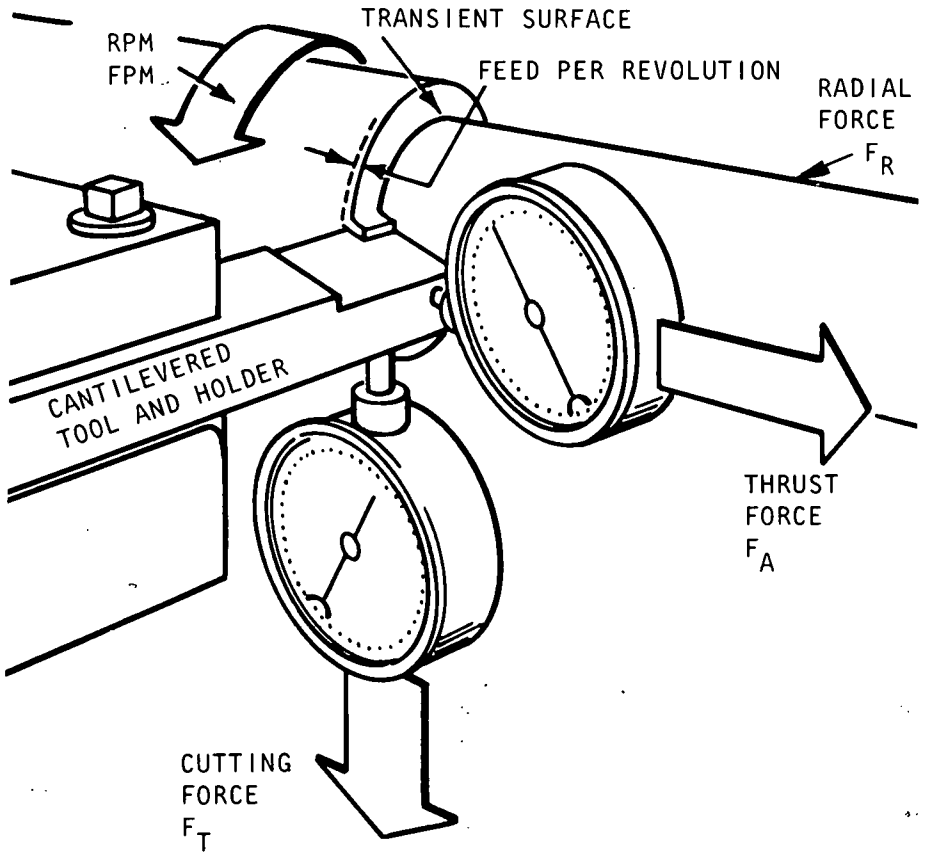

Figure 29. Forces on Cutting Tool During Turning[12]

samples produced at each cutting condition were used to provide ten readings for each combination. Tables 5 and 6 were prepared on the assumption that interactions were not significant.

Burr Height

In the previous study, the SCEA, the depth-of-cut, and the feedrate were shown to be highly significant in determining burr height for 303Se stainless steel. This was reaffirmed in this study (Table 5). Beryllium-copper specimens did not appear to be affected by the SCEA, although the other materials were. The indication that the ECEA and the end relief (ERF) affected the burr height is not compatible with the theory of burr formation. This particular indication of significance probably was due to the higher-order interactions of the other variables.

As shown in Table 3, the burr height varied from 30.48 to 492.8 μm (0.0012 to 0.0194 inch) when the average of all cuts were taken.

Table 4. Unit Power (W_N) Values

Material	Unit Power: Experimental Values: Average* ($W/cm^3/s$; $HP/in.^3/min$)	Unit Power: Experimental Values: Tool 1** ($W/cm^3/s$; $HP/in.^3/min$)	Unit Power: Handbook Value*** ($W/cm^3/s$; $HP/in.^3/min$)
303Se	3.57 (4.7)	2.96 (3.9)	0.99 (1.3)
15-5PH	2.36 (3.1)	1.75 (2.3)	1.06 (1.4)
BeCu	1.29 (1.7)	0.91 (1.2)	0.76 (1.0)
Type A*	1.98 (2.6)	1.52 (2.0)	1.52 (2.0)
Type B**	3.80 (5.0)	3.34 (4.4)	1.90 (2.5)

*Glass sealing alloy, 53Fe-29Ni-17Co, SAE unified number K94610.
**2V permendur high magnetic permeability steel, 49Fe-49Co-2V, SAE unified number K95100.
***Average values based on 8 tools; grossly exaggerated data are excluded.
****Values obtained from Tool 1 (Level 1 of all tool angles and depth-of-cut shown in Table 3).
*****Traditional-unit values from Machining Data Handbook.[12]

While the elongation of a workpiece is one key to burr size, in this study, the strain-hardening exponent proved to be the best key (Figures 31 and 32). Appendix Table A-3 lists the workpiece properties, and the data for individual tools are presented in Appendix Tables A-4 through A-8.

Burr Thickness

The previous study using 303Se stainless steel indicated that burr thickness is a function of the SCEA, the depth-of-cut, and the feedrate. For depths-of-cut having the same magnitude as the nose radius, the SCEA should not have any noticeable influence. This is basically confirmed by this study (Table 6). Again, the indication that the ECEA and the ERf influence burr thickness is not consistent with the theory of burr formation.

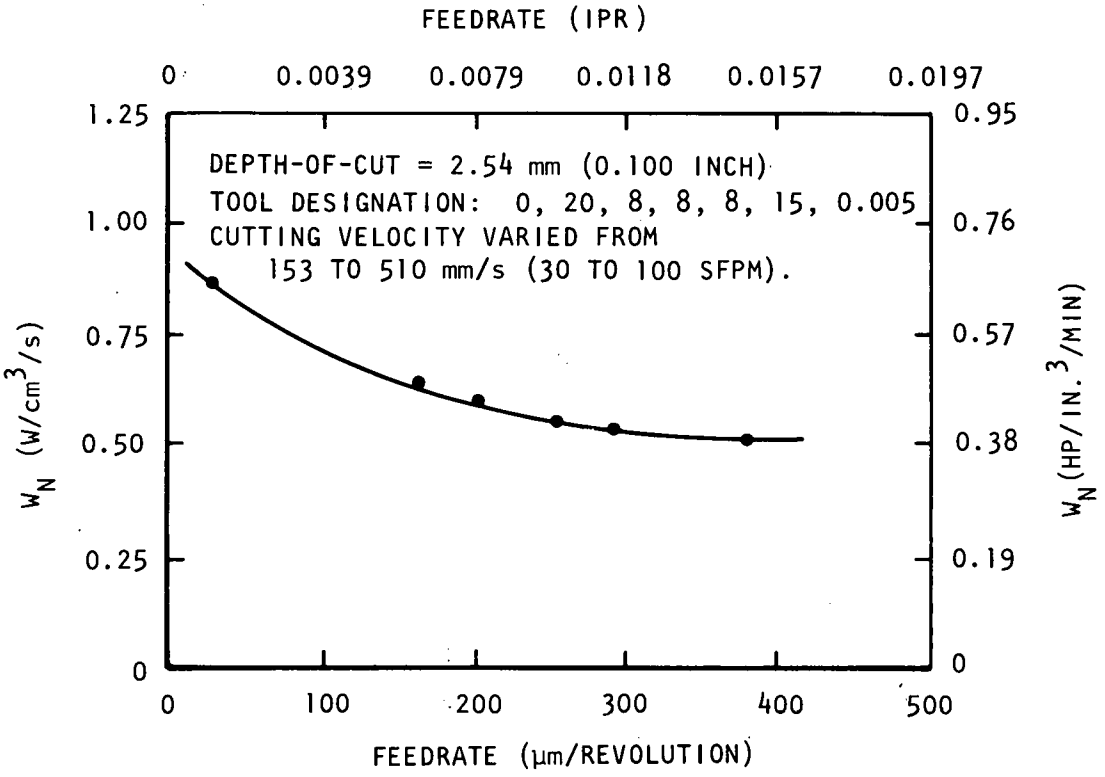

Figure 30. Effect of Feedrate on Unit Power for HSS Tool in 1020 Steel

As shown in Table 3, burr thickness varied from 40.6 to 114.3 μm (0.0017 to 0.0045 inch) when average properties were calculated. Burr thickness is a linear function of the strain-hardening exponent (Figure 32). It also appears to be related to the elongation of the workpiece (Figure 31).

For miniature precision components, burr thickness must be kept less than 76.2 μm (0.003 inch) in order to maintain part dimensions during a deburring operation. The thinner a burr, the easier it is to remove.

When the five materials are ranked by conventional machinability rankings, cutting force, and burr size, few relationships are immediately obvious from the results (Table 7). The material that was most difficult to machine, 15-5PH stainless steel, produced the smallest burrs. This result, however, is consistent with the results shown in Figure 31.

Many of the low-machinability ratings are for hardened materials having low ductility. Hardened tool steel is one such example.

Table 5. ANOVA Summary for Burr Height

Effect	Material				
	303Se	15-5PH	BeCu	Type A†	Type B††
ECEA (A)		**		***	*
ERf (B)		*	***	***	
BR (C)		*		***	
SR (D) [AC]****	**	***		***	
SCEA (E) [BC]	*	***		***	*
Depth-Of-Cut (F) [ABC]	**			***	***
ECEA x ERf (AB)	*	***	*	***	

*Significant effect at 95-percent confidence level.
**Significant effect at 99-percent confidence level.
***Significant effect at a confidence level exceeding 99 percent.
****[ ] Equated to the factor to generate the fractional replicate.
†Glass sealing alloy, 53Fe-29Ni-17Co, SAE unified number K94610.
††2V permendur high magnetic permeability steel, 49Fe-49Co-2V, SAE unified number K95100.

Table 6. ANOVA Summary for Burr Thickness

Effect	Material				
	303Se	15-5PH	BeCu	Type A†	Type B††
ECEA (A)		***	*		*
ERf (B)	**		**		
BR (C)					
SR (D) [AC]****		**			
SCEA (E) [BC]		***			*
Depth-Of-Cut (F) [ABC]	**	*			***
ECEA x ERf (AB)		**	**		

*Significant effect at 95-percent confidence level.
**Significant effect at 99-percent confidence level.
***Significant effect at a confidence level exceeding 99 percent.
****[ ] Equated to the factor to generate the fractional replicate.
†Glass sealing alloy, 53Fe-29Ni-17Co, SAE unified number K94610.
††2V permendur high magnetic permeability steel, 49Fe-49Co-2V, SAE unified number K95100.

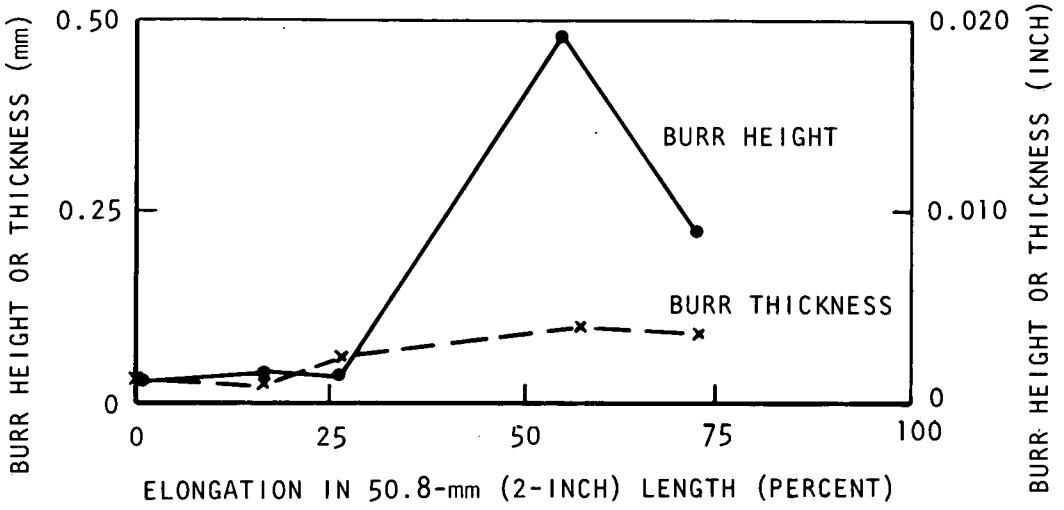

Figure 31. Effect of Elongation on Burr Height or Thickness

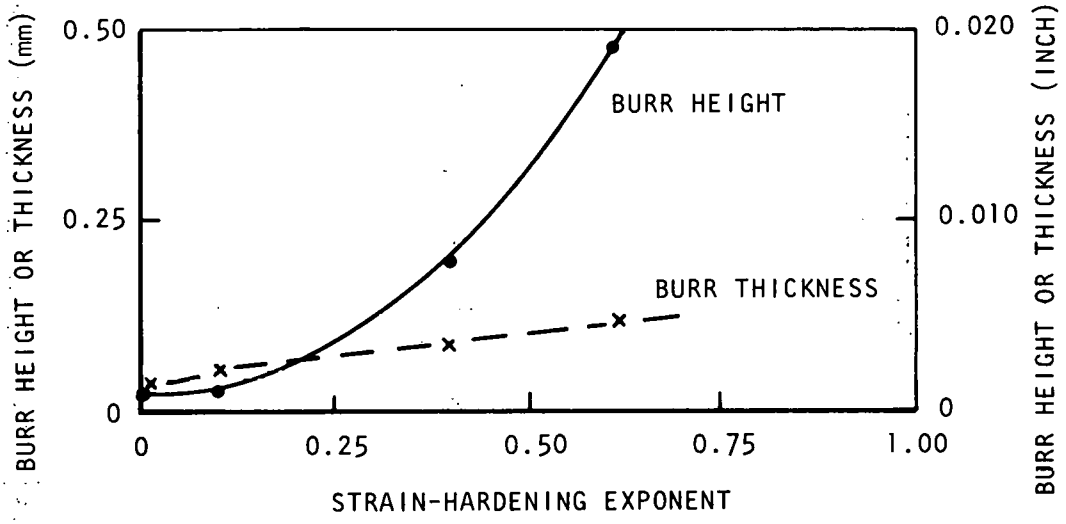

Figure 32. Effect of Strain-Hardening Exponent on Burr Height or Thickness

Large burrs cannot form unless the material is ductile. Cutting forces alone are not a good indicator between different materials because, as shown in Equations 1 through 4, the ratio of cutting forces or pressure to yield strength is the significant relationship.

Table 7. Results Ranked by Material, Using Optimum Tool Geometry

Measured Variable and Measuring Units	Material Ranking				
Handbook Recommended	Decreasing Recommended Speed				
Cutting Speed	BeCu	Type A*	303Se	Type B**	15-5PH
mm/s	1275	729	510	306	245
SFPM	250	143	100	60	48
	Properties Increase				
Cutting Force	BeCu	Type A	15-5PH	303Se	Type B
N	21.8	32.0	44.5	55.2	76.5
Pounds	4.9	7.2	10.0	12.4	17.2
Burr Height	15-5PH	Type B	BeCu	Type A	303Se
μm	0	10.2	11.7	68.8	245.6
Inch	0	0.0004	0.00046	0.00271	0.00967
Burr Thickness	15-5PH	Type B	BeCu	Type A	303Se
μm	0	11.2	22.4	80.3	88.4
Inch	0	0.00044	0.00088	0.00316	0.00348

*Glass sealing alloy, 53Fe-29Ni-17Co, SAE unified number K94610.
**2V permendur high magnetic permeability steel, 49Fe-49Co-2V, SAE unified number K95100.

The fact is interesting to note that for the Poisson burrs in this study, thick burrs also indicated higher burrs (Table 7). The data shown for force and burr size in Table 7 are for the tool geometry (Tool 3) that generally produced the lower forces, the smaller burrs, and the smoother surfaces.

The second reason for the apparent inconsistencies is that the hardnesses of the materials used in this study were different from those on which machinability ratings were based. For example, 15-5PH stainless steel in the H900 condition has a hardness of R_C42, while the hardness of the material used in this study was only R_C30. Machinability ratings are typically given for only one material condition; thus they often do not reflect the conditions that are encountered in practice.

Tool Wear and Its Effects

Tool wear was monitored during this study to determine whether conventional definitions of tool life had any correlation with the parameters that were of interest. In addition, a knowledge of how the observed results were influenced by tool wear was desired. Because the tool wear was not expected to be as great as that which normally is encountered in conventional machinability tests, it was only checked after each group of 10 specimens had been produced. Since each tool produced only 10 specimens, one group of readings was obtained for each set of machining conditions.

Although tool wearlands were measured during this study, there was no obvious correlation between the wearland size and either the burr size or the cutting force. For 28 of the 160 combinations related to burrs, the observed wear relationship was of the following form.

$$Y = a_1 + a_2X, \tag{15}$$

where

Y = the burr size or cutting force,

X = the number of specimens machined,

a_1 = a constant, and

a_2 = a constant.

The equation can be made more explicit by substituting the inches-of-cut or the time-in-cut for each specimen to produce the following two equations:

$$Y = a_1 + a_2\left(\frac{T}{0.432}\right); \quad (16)$$

and

$$Y = a_1 + a_2\left(\frac{L}{5.625}\right); \quad (17)$$

where

T = the time-in-cut, in minutes; and

L = the length-of-cut, in inches.

The a_1 and a_2 constants for the combinations in which linear trends existed are presented in Appendix Table A-9.

In general, the conclusion would have to be reached that tool wear affected the measured properties very little. Specific tools did exhibit wear in some specific materials, as evidenced by Table A-9.

Burrs on Production Parts

Most of the burrs that are found on turned production parts are smaller than those that were found in the two described tests. Figure 33, however, shows one exception; the burrs shown were produced with typical turning tools in a roughing cut. The material consisted of a 152.4-mm-diameter (6-inch) bar of 304 stainless steel.

Figure 34 shows an enlarged view of a portion of a miniature precision part containing a typical facing burr produced by an automatic screw machine. These roll-over-type burrs, produced as illustrated in Figure 14, are less than 25.4 μm (0.001 inch) high on this R_C42 stainless steel part.

Figure 35 shows a typical miniature precision component that is produced at Bendix through the use of automatic screw machines and, together with Table 8, it describes machining conditions that are used and the resulting burrs. A typical miniature precision part that is produced on chucker lathes is similarly described in Figure 36 and Table 9. As indicated, the necessity for maintaining close diameter tolerances requires the use of sharp tools and low feedrates, which also helps to keep the burrs small.

The width of the cutoff projection is equal to the width of the cutoff tool. This burr cannot be prevented unless the part is constrained until the cutoff has been completed. While this can be done on most screw machines, it commonly is done on only the multiple spindle automatic screw machines.

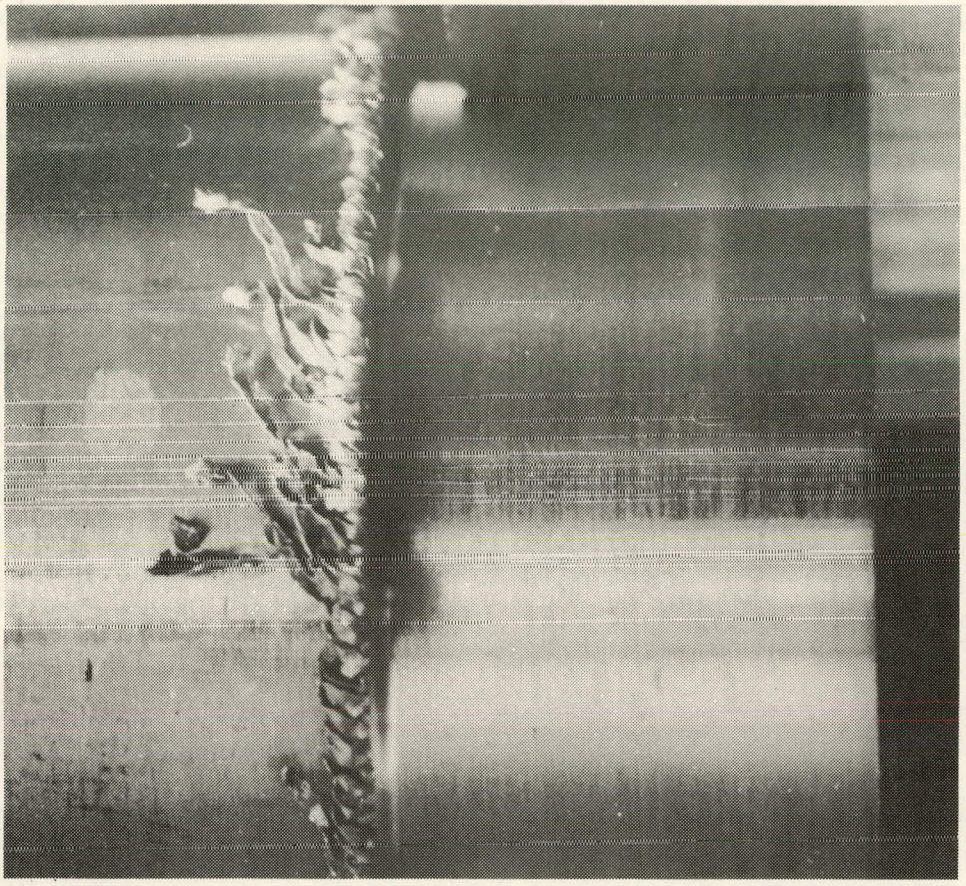

Figure 33. Unusually Long Burrs on Large Bar of 304 Stainless Steel

Analysis of Published Literature

Okushima appears to be the first individual to have studied burrs produced by turning and planing.[13] His study of burrs that occur at the sides of the workpiece (Figure 37) indicate that edge conditions can assume any of the four different configurations shown in Figure 38. The flow-type edge condition (Figure 38A) is the Poisson burr that is described in this report. Okushima found these burrs on low-carbon steel, chrome steel, and yellow brass when dull tools were used.

The whisker-type burr (Figure 38B) was found when negative-rake tools were used. These burrs, which somewhat resemble chips, often wrap around the workpiece to produce a condition such as that shown in Figure 39.

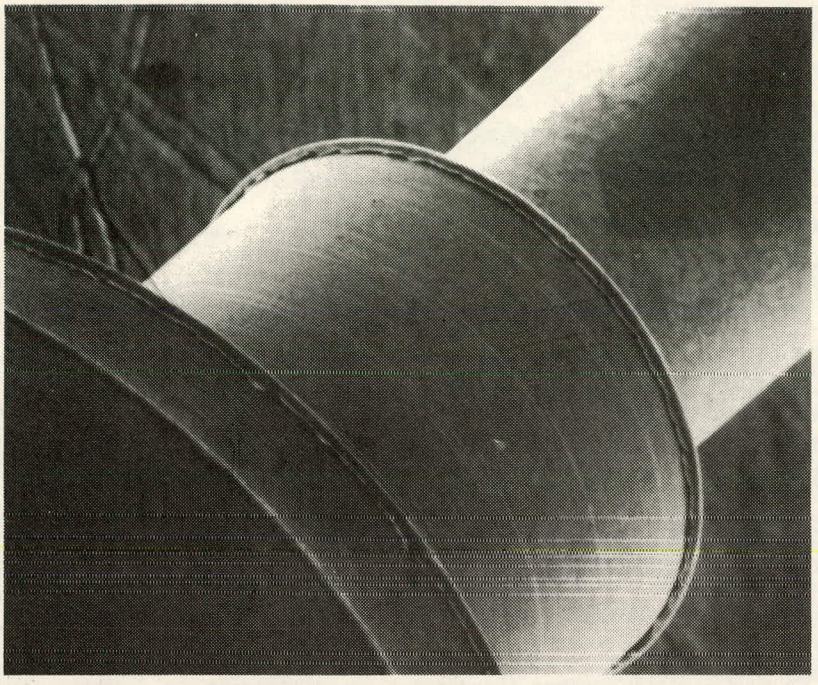

Figure 34. SEM Photograph of Facing Burr on Miniature Precision Part Produced by Swiss Automatic Screw Machine (Magnification: 100X)

The tear-type edge (Figure 38C) is produced as the result of nonuniform shearing during the cutting operation. Apparently, a built-up edge (BUE) occurs and intermittently breaks free of the part. When the BUE becomes too large, tearing takes place, rather than normal shearing. This combination allows the BUE to weld to the sides of the workpiece and produces the nonuniform edge.

The cavity-type edge (Figure 38D) is similar to the condition that is found when splinters are torn from the edges of wood boards.

The height of the burrs found on yellow-brass workpieces increased with a decreased rake angle and with an increased depth-of-cut. At a cutting velocity of 5.2 m/minute (17 feet/minute) and a depth-of-cut of 0.1 mm (0.004 inch), a 30-degree rake angle produced essentially no burrs, while a -20-degree angle produced burrs that were 0.75 mm (0.030 inch) high. Burr height increased linearly when a 0-degree rake angle was used and the depth-of-cut was increased to 0.3 mm (0.012 inch). At the 0.3-mm depth-of-cut, the burr height was 0.4 mm (0.016 inch).

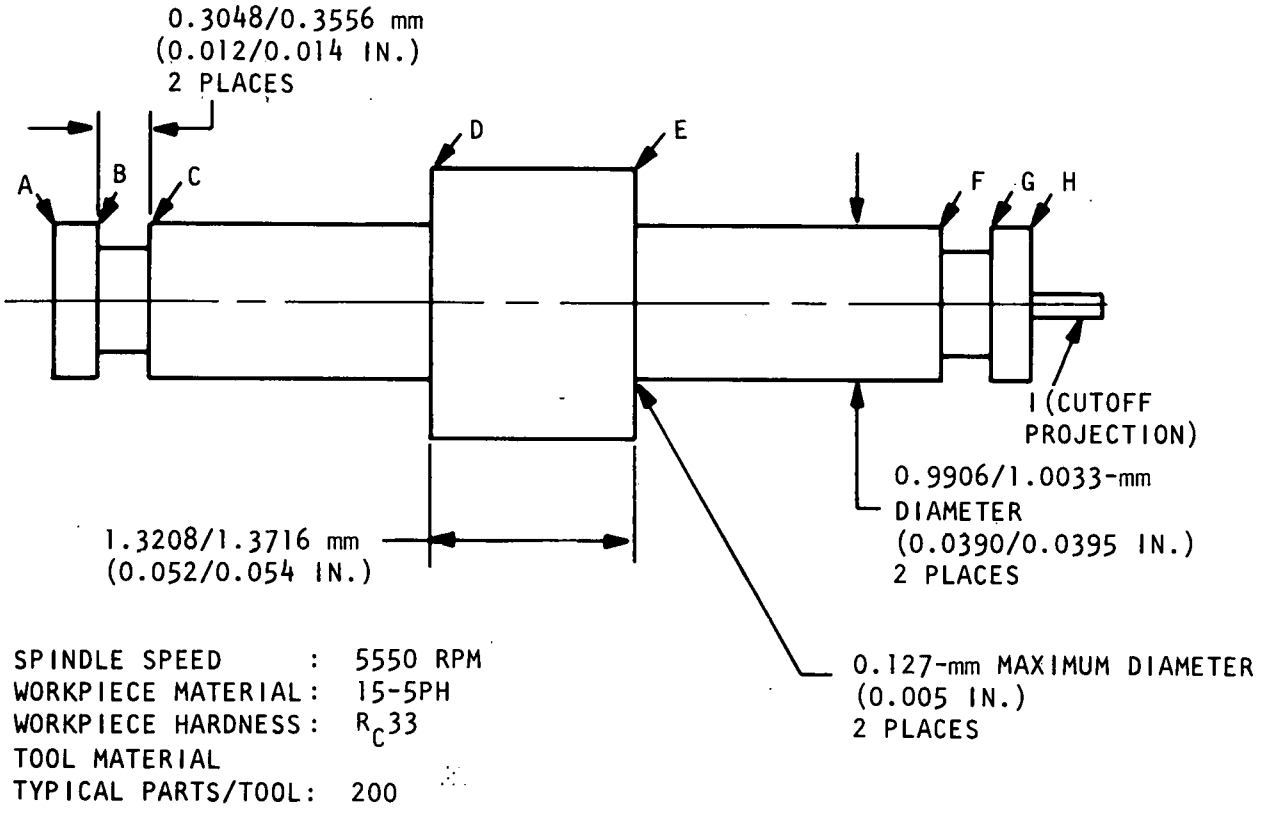

Figure 35. Miniature Precision Part Produced on a Swiss Automatic Screw Machine

The whisker-type burrs described by Okushima[13] were observed during this study after turning 303Se stainless steel (Figure 39). While these burrs are not common, they do occur frequently with 303Se stainless steel when the tool geometry differs significantly from the recommended geometry. The tear-type edge described by Okushima, not to be confused with the tear burr described in this report, occurs only on materials which tend to produce a built-up edge. The cavity-type edge can be found on several brittle materials such as cast iron or 2V permendur high magnetic permeability steel.

The burr heights observed by Okushima on brass were much larger than would be expected to occur. The observation that burr height was a function of depth-of-cut and rake angle is in agreement with the results described in this study.

Masuda[14] and others[15-17] have pointed out that minute burrs occur on all turned surfaces (as differentiated from edges). Metal flows laterally along the crest of each scallop produced by the nose of the cutting tool to produce miniature Poisson burrs

Table 8. Typical Burrs Produced on Swiss Automatic Screw Machines

Edge*	Tool Feedrate (μm/Rev; IPR)	Burr Type	Burr Size** Height (μm; Inch)	Burr Size** Thickness (μm; Inch)
A	10.2 (0.0004)	Poisson	0 (0)	0 (0)
B	5.1 (0.0002)	Tear	10.2, 12.7 (0.0004, 0.0005)	12.7, 12.7 (0.0005, 0.0005)
C	5.1 (0.0002)	Tear	0, 5.1 (0, 0.0002)	0, 30.5 (0, 0.0012)
D	10.2 (0.0004)	Poisson	15.2, 25.4 (0.0006, 0.0010)	25.4, 38.1 (0.0010, 0.0015)
E	10.2 (0.0004)	Poisson	17.8, 20.3 (0.0007, 0.0008)	25.4, 45.7 (0.0010, 0.0018)
F	5.1 (0.0002)	Tear	20.3, 22.9 (0.0008, 0.0009)	33.0, 33.0 (0.0013, 0.0013)
G	5.1 (0.0002)	Tear	10.2, 27.9 (0.0004, 0.0011)	20.3, 30.5 (0.0008, 0.0012)
H	10.2 (0.0004)	Poisson	22.9, 30.5 (0.0009, 0.0012)	25.4, 25.4 (0.0010, 0.0010)
I	10.2 (0.0004)	Cutoff	883.9 (0.0348)	218.4 (0.0086)

*Refer to Figure 35 for location of edges; none of the edges were chamfered on the machine.
**Most entries show two measurements that were made.

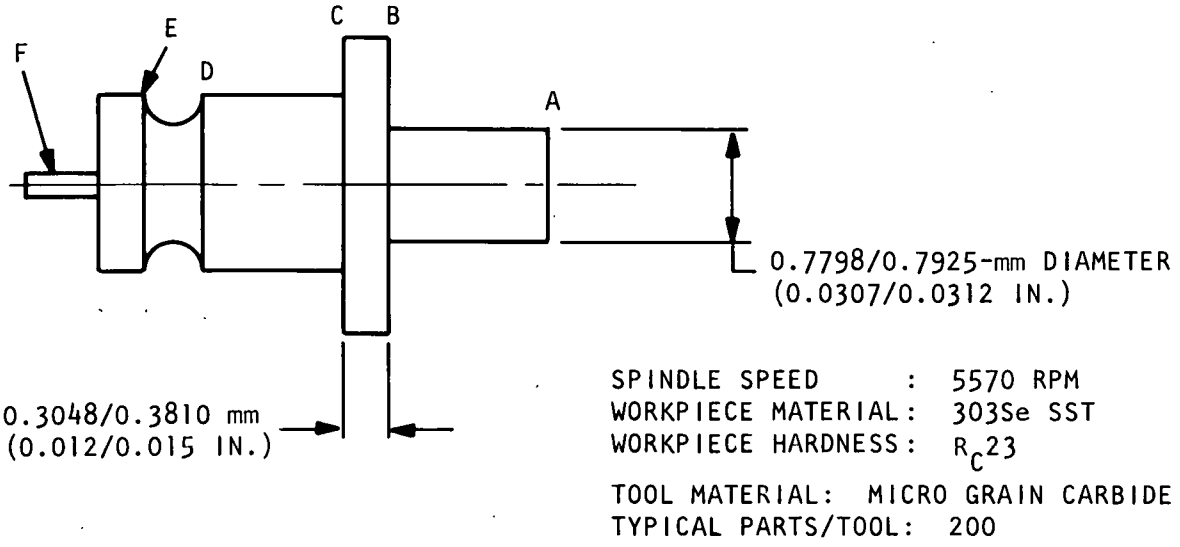

Figure 36. Miniature Precision Part Produced on a Chucker Lathe

(Figure 40). These burrs, which affect surface-finish measurements, typically are from 0.127 to 0.508 μm (5 to 20 microinches) in height. Since these burrs can be seen only under a magnification of 100 to 400X and they can be easily removed by most surface-finishing processes, they do not create a problem in normal precision machining operations.

The Impact of Burr Size on Deburring

Burr size is a major factor in the cost of deburring. Minute burrs can be easily and quickly removed by any of the 24 principal deburring processes without affecting part dimensions or finishes. Burrs that are thick and high, however, can be removed only by specially designed mechanized processes or hand-deburring operations when precision tolerances and finishes must be maintained on parts.

For example, consider the burrs produced on a 9.525-mm-diameter (0.375 inch), 9.525-mm-long cylinder in a cutoff operation. If this cylinder were of a 300-series stainless steel with a hardness of R_C32, deburring in a centrifugal barrel tumbler at 15 g's with N14 aluminum oxide nuggets would reduce the burr size by the amount shown by the following equation.

Table 9. Typical Burrs Produced on Chucker Lathes

Edge*	Burr Size** Height (μm; Inch)	Thickness (μm; Inch)
A		
B***	0 (0)	0 (0)
C	30.5, 43.2 (0.0012, 0.0017)	38.1, 40.6 (0.0015, 0.0016)
D	27.9, 33.0 (0.0011, 0.0013)	43.2, 48.3 (0.0017, 0.0019)
E	7.6, 7.6 (0.0003, 0.0003)	10.2, 12.7 (0.0004, 0.0005)
F	769.6 (0.0303)	477.5 (0.0188)

*Refer to Figure 36 for location of edges; all operations were hand-fed; edges were not chamfered on the machine unless otherwise indicated.
**Most entries show two measurements that were made.
***Edge B was chamfered on the machine.

$$\Delta h = 4.69 w^{-1.2} t^{0.713 w^{0.169}} \times 10^{-4}, \quad (18)$$

where

Δh = the change in burr height (in inches),

w = the initial burr thickness (in mils), and

t = the time in the harperizer (in minutes).

As shown in Figure 41, burrs 25.4 μm (0.001 inch) or less in thickness are reduced in height much faster than are the thicker burrs. If the burr were also short, very little time would be required to remove it under the conditions indicated. For these same conditions, the change in part dimensions can be calculated from the following equation.

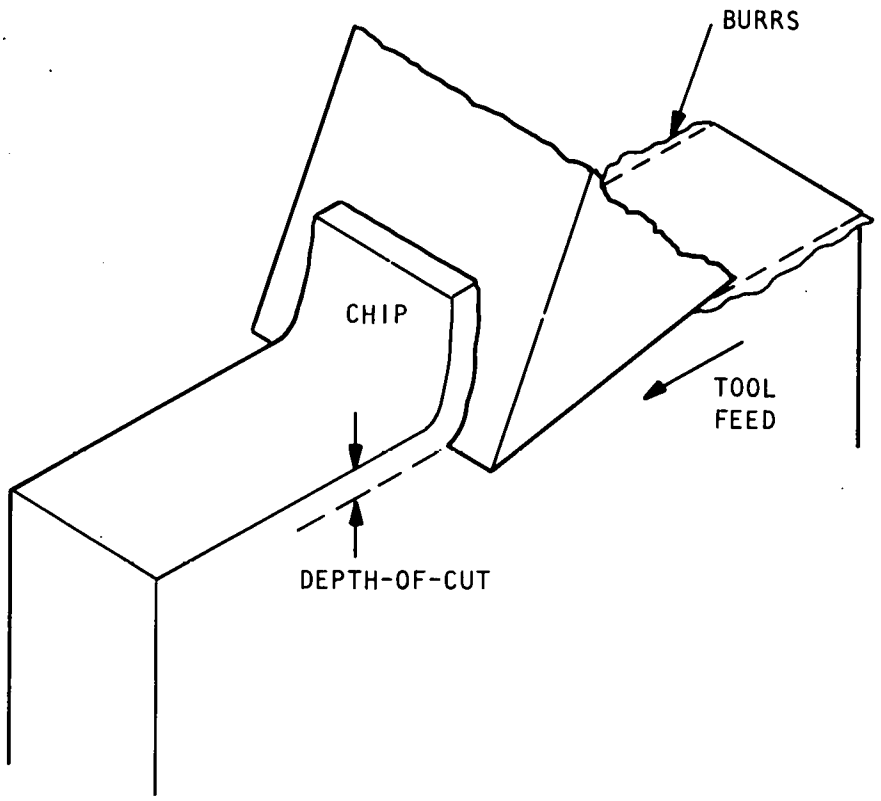

Figure 37. Poisson Burrs Produced by Planing

$$\Delta D = -0.016D^{0.306}t \times 10^{-3}, \quad (19)$$

where

ΔD = the change in the diameter of the cylinder (in inches), and

D = the initial cylinder diameter (in inches).

Note that this equation is only valid for cases in which the length and diameter of the cylinder are equal. From the equation, the workpiece diameter can be seen to decrease linearly with an increase in the deburring time.

As a general rule of thumb, a 25.4-μm-high by 25.4-μm-thick (0.001 by 0.001 inch) burr on a small steel part can be removed without decreasing the part size more than 2.54 μm (0.0001 inch). In addition to removing the burr, such processes as harperizing will produce an edge radius of 50.8 to 127.0 μm (0.002 to 0.005 inch). If larger burrs are present, they cannot be removed while maintaining an edge radius of 50.8 μm.

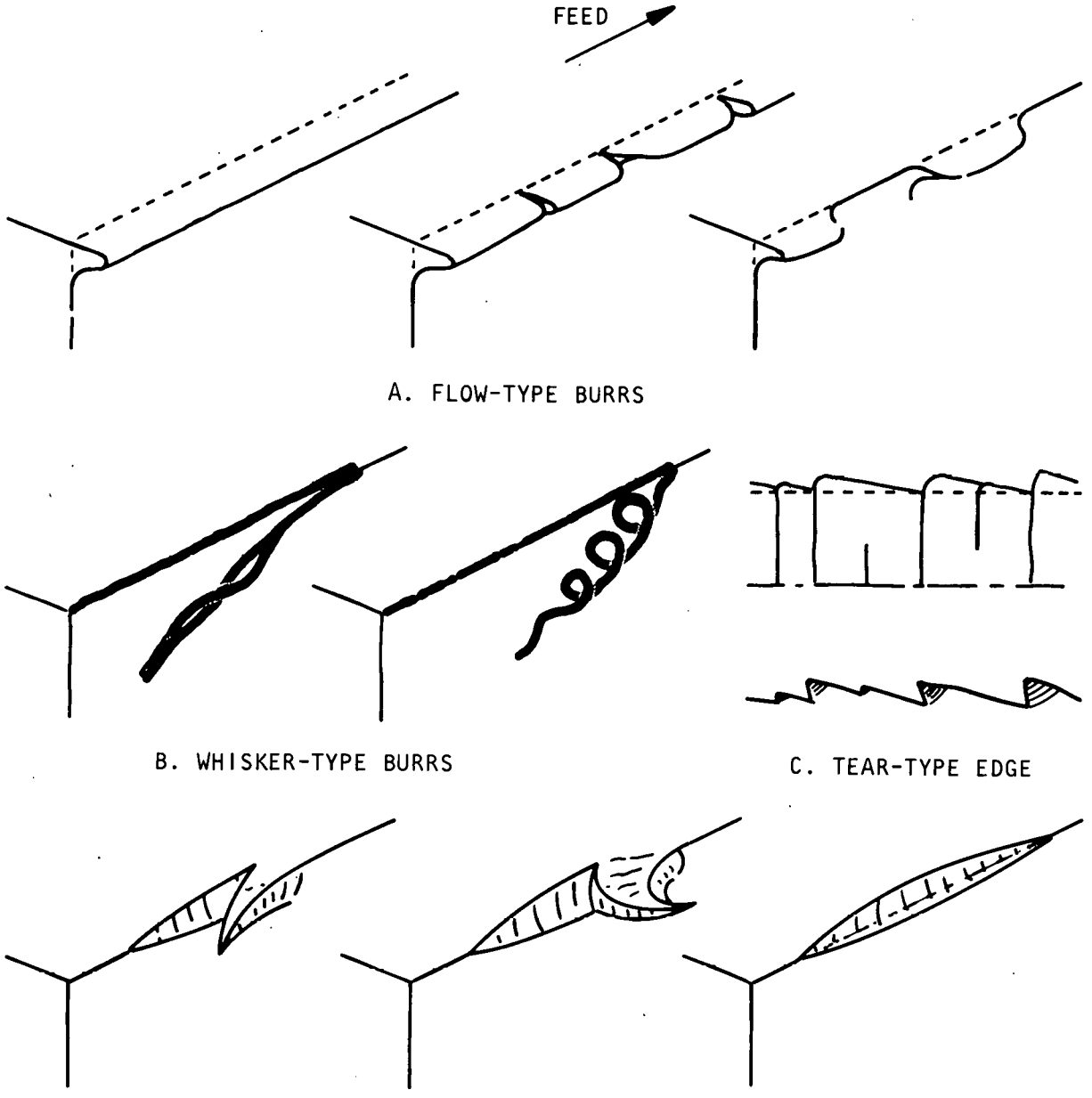

Figure 38. Types of Edge Conditions Produced in Turning Operations[13]

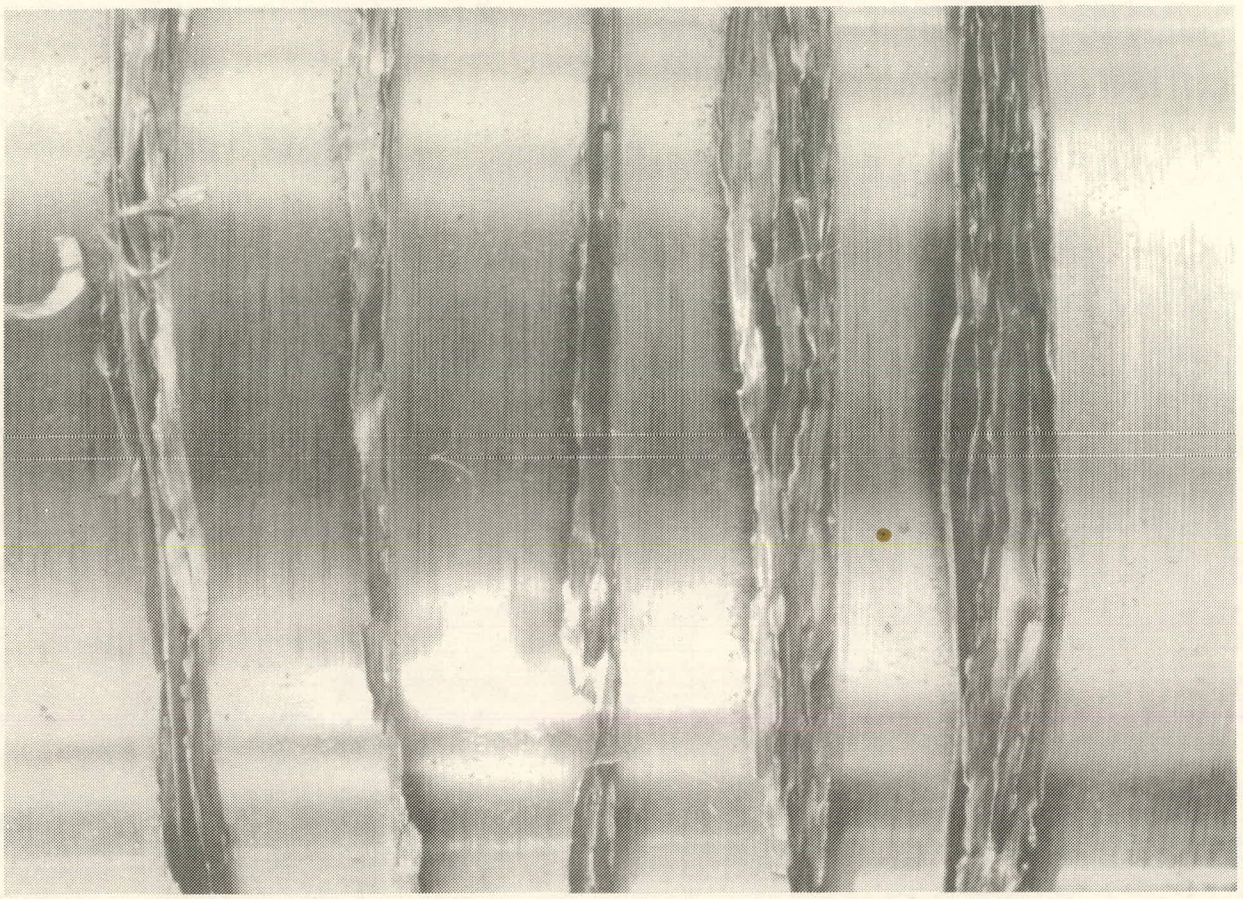

Figure 39. Whisker-Type Burrs Produced From 303Se Stainless Steel

Conventional loose-abrasive deburring processes, when used to remove large burrs, create large edge radii. Thus when the tolerances for miniature parts limit stock losses to 2.54 μm (0.0001 inch) or less and edge radii to a maximum of 50.8 to 76.7 μm (0.002 to 0.003 inch), the initial burr size must be in the order of 25.4 μm (0.001 inch). Larger burrs require hand-deburring which is time-consuming and not as repeatable as many of the mechanized processes.

Equation 19 illustrates one other aspect of the influence of the workpiece on deburring: for a given set of conditions, small parts receive significantly less deburring action than do large parts. When parts are only 0.5 mm (0.020 inch) in diameter, the burrs must be kept small so that deburring can be accomplished in a matter of minutes rather than days.

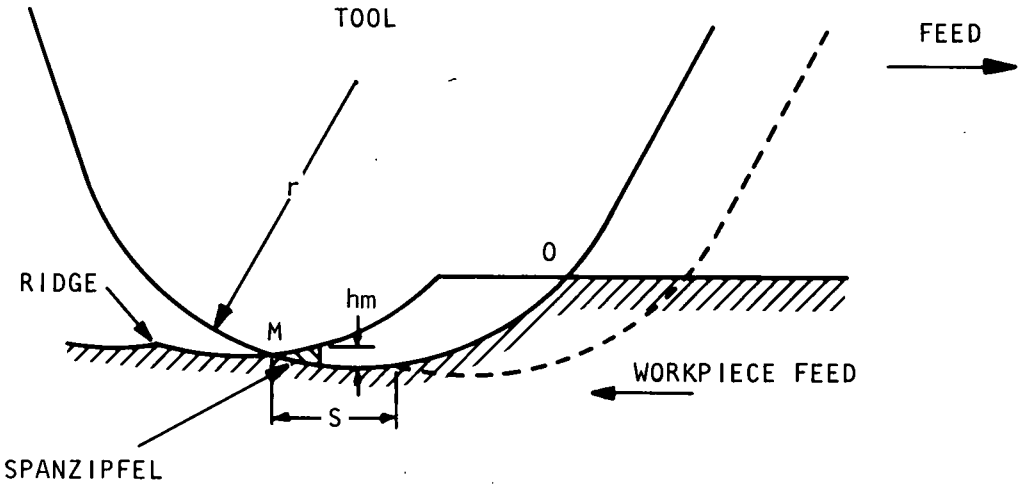

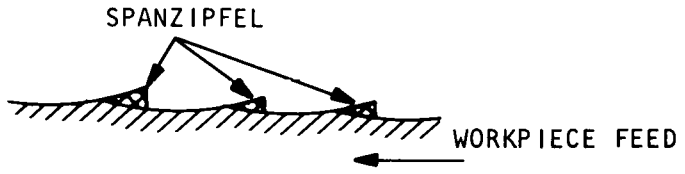

EFFECT OF SPANZIPFEL

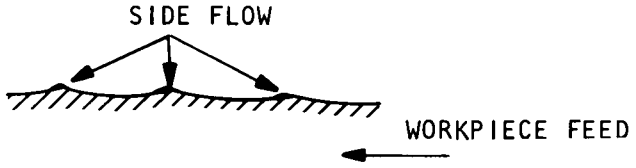

EFFECT OF SIDE FLOW ON ROUGHNESS

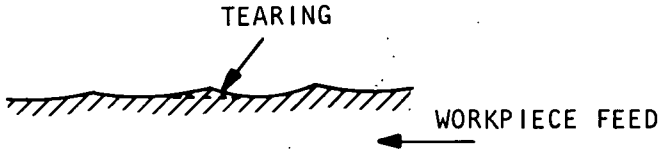

EFFECT OF TEARING

Figure 40. Effect of Various Factors on the Profile of the Ridge Left by Turning[17]

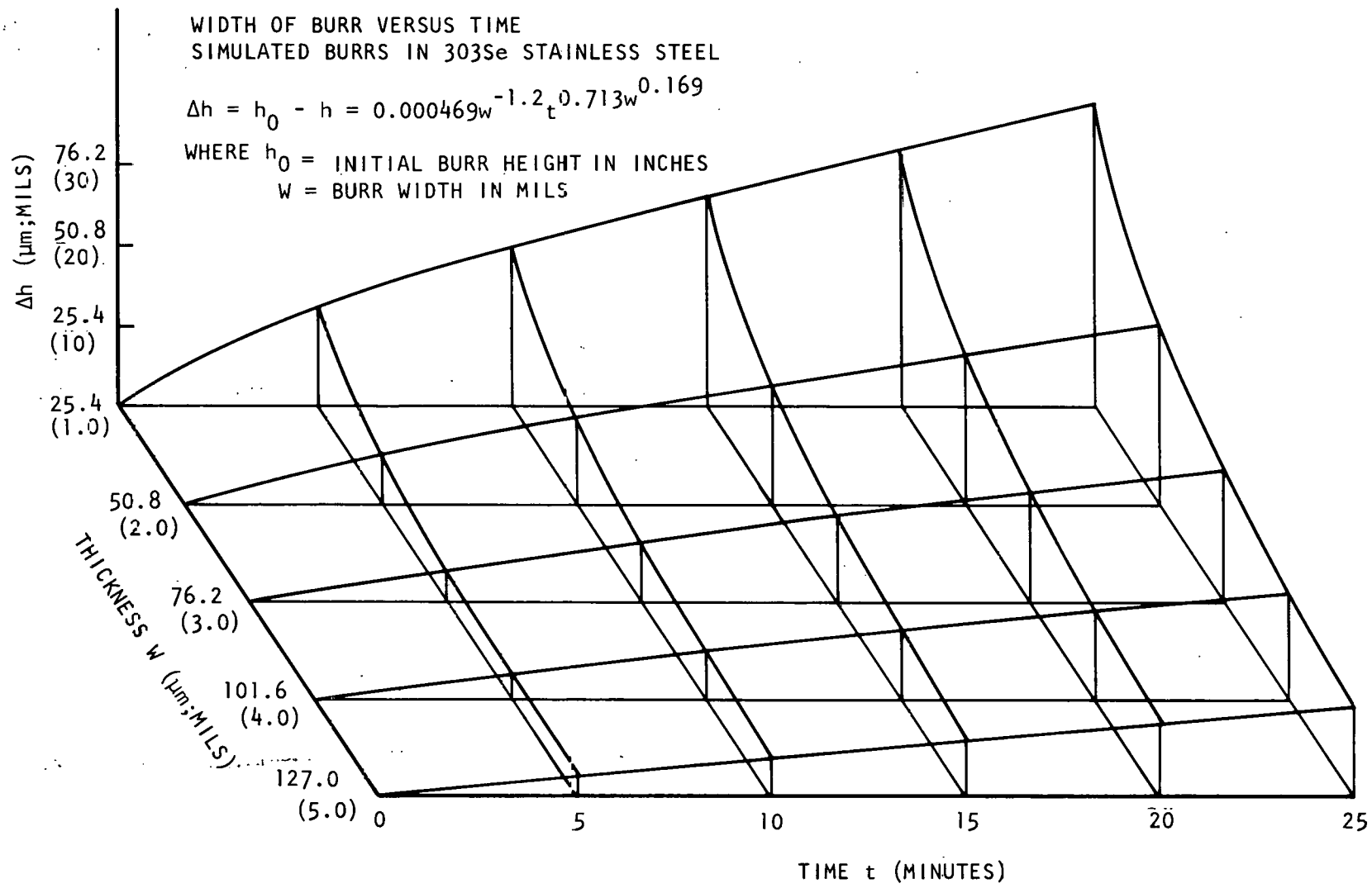

Figure 41. Reduction of Burr Height by Centrifugal Barrel Tumbling

While the relationships shown in Equations 18 and 19 are only valid for the conditions described, the basic relationships are valid for all deburring processes. The effect of deburring time on part size can be compensated for by increasing the initial part size, but the required coordination is cumbersome to maintain in low-volume, job-shop situations. Furthermore, the repeatability of many deburring processes is less than that which is required for some parts. For example, centrifugal barrel tumbling under certain situations has a size-change standard deviation (σ) of 0.51 μm (0.000020 inch). While 95-percent limits (2σ) of $\pm$1.02 μm ($\pm$0.000040 inch) are adequate for most parts, they are inadequate for parts having a tolerance of $\pm$1.27 μm (0.000050 inch).

The large burrs described in this report are seldom seen by anyone except the lathe operator, who frequently removes them while making the part. Common practice consists of holding a file or sandpaper against each edge while the part is still chucked in the lathe collet. This hand-deburring operation removes all or most of the burr.

In the production of miniature parts on automatic screw machines, the described hand-deburring technique is not feasible. With these machines, unused tool positions often are used to chamfer the part edges to remove large burrs. When the allowable edge-break or chamfer is only 50.8 μm (0.002 inch) or less, this method becomes difficult to control. In addition, few of the machines that are used at Bendix to produce miniature precision parts have extra tool positions to devote to this purpose.

ACCOMPLISHMENTS

The effect of tool geometry, feedrate, and spindle speed on burr size has been documented for turning operations. Feedrate, back-rake angle, and side-cutting edge angle have been shown to be the more significant factors influencing the size of the burrs produced.

Four different types of burrs occur on most turned parts. An explanation of how these burrs are produced and their impact on deburring efforts has been developed.

REFERENCES

[1]L. K. Gillespie, *The Formation and Properties of Machining Burrs*, MS Thesis, Utah State University, Logan, Utah, 1973.

[2]L. K. Gillespie, *The Effects of Reaming Variables on Burr Properties* (Topical Report). Bendix Kansas City: BDX-613-1083 (Rev.), September, 1974 (Available from NTIS).

[3]L. K. Gillespie, *Properties of Burrs Produced by Ball Broaching* (Topical Report). Bendix Kansas City: BDX-613-1084 (Rev.), April, 1975 (Available from NTIS).

[4]L. K. Gillespie, *Burrs Produced by Drilling* (Topical Report). Bendix Kansas City: BDX-613-1248, August, 1976 (Available from NTIS).

[5]L. K. Gillespie, *Effects of Drilling Variables on Burr Properties* (Topical Report). Bendix Kansas City: BDX-613-1502, September, 1976 (Available from NTIS).

[6]L. K. Gillespie, *Burrs Produced by End Milling* (Topical Report). Bendix Kansas City: BDX-613-1503, October, 1976 (Available from NTIS).

[7]L. K. Gillespie, *Burrs Produced by Side-Milling Cutters* (Topical Report). Bendix Kansas City: BDX-613-1303 (Rev.), November, 1975 (Available from NTIS).

[8]L. K. Gillespie, *Burrs Produced by Grinding* (Topical Report). Bendix Kansas City: BDX-613-1372, August, 1976 (Available from NTIS).

[9]L. K. Gillespie and P. T. Blotter, *The Formation and Properties of Machining Burrs*, ASME Paper 75-PROD-J, 1975.

[10]L. K. Gillespie, *The Formation and Properties of Burrs*, SME Paper MRR 75-03, April, 1975.

[11]L. K. Gillespie, *The Effect of Cutting Edge Radius on Poisson Burr Properties*, SME Paper, MR 74-990, 1974.

[12]*Machining Data Handbook*, 2nd edition. Cincinnati, Ohio: Metcut Research Associates, 1971.

[13]Keiji Okushima and Katsundo Hizomi, "Side Flow of Metal Furing Machining: I- for Orthoginal Cutting," *Seimitsu Kikai*, Volume 24, Number 8, 1958, pp 16-20 (in Japanese).

[14]Kazuaki Masuda, "Some Observations of the Surface Roughness of Mild Steel Finished by Turning," *Bulletin of the Japan Society of Mechanical Engineers*, Volume 13, (57), 1970, pp 462-473.

[15]Kozo Kishi and Hiroshi Eda, "Analysis of Transition Structure of the Machined Surface Layer Due to Built-Up Edges," *Journal of The Japan Institute of Metals*, Volume 36, Number 1, January, 1972, pp 14-21.

[16]P. Dinichert and others, "The Evaluation of the Surface by Roughness Measurement Situation 1973," *Annals of the CIRP*, Volume 22, Number 2, 1973.

[17]M. S. Selvam and V. Radhakrishnan, "Effect of Side Flow on the Straightness of the Ridge and the Surface Roughness," *International Journal of Machine Tool Design and Research*, Volume 13, 1973, pp 243-255.

Appendix

DATA TABLES

Table A-1. Results of Turning Tests*

Order of Cut	SCEA (Degrees)	Depth-Of-Cut (mm; Inch x 10^{-3})	Feedrate (μm/Rev; IPR)	Burr Properties** Height (μm; Inch x 10^{-4})	Hardness (Knoop)	Thickness (μm; Inch x 10^{-4})	Workpiece Hardness (Knoop)
1	17-1/2	1.016 (40)	53.3 (0.0021)	10.2 (4) 0 (0) 20.4 (8)		0 (0)	
2	17-1/2	1.778 (70)	53.3 (0.0021)	10.2 (4) 7.6 (3) 17.8 (7)		20.4 (8) 17.8 (7)	
3	17-1/2	2.540 (100)	53.3 (0.0021)	27.9 (11) 40.6 (16) 38.1 (15)		20.4 (8)	
4	17-1/2	1.016 (40)	109.2 (0.0043)	22.9 (9) 15.2 (6) 17.8 (7)		15.2 (6) 15.2 (6)	
5	17-1/2	1.778 (70)	109.2 (0.0043)	2.5 (1) 2.5 (1)		17.8 (7) 12.7 (5)	
6	17-1/2	2.540 (100)	109.2 (0.0043)	61.0 (24) 48.3 (19) 53.3 (21)		25.4 (10) 30.5 (12)	
7	17-1/2	1.016 (40)	165.1 (0.0065)	22.9 (7) 10.2 (4) 7.6 (3)		20.4 (8) 12.7 (5)	
8	17-1/2	1.778 (70)	165.1 (0.0065)	2.5 (1) 0 (0) 2.5 (1)		33.0 (13) 12.7 (5)	

Table A-1 Continued. Results of Turning Tests*

Order of Cut	SCEA (Degrees)	Depth-Of-Cut (mm; Inch x 10^{-3})	Feedrate (μm/Rev; IPR)	Burr Properties** Height (μm; Inch x 10^{-4})	Hardness (Knoop)	Thickness (μm; Inch x 10^{-4})	Workpiece Hardness (Knoop)
9	17-1/2	2.540 (100)	165.1 (0.0065)	10.2 (4) 10.2 (4) 5.1 (2)		30.5 (12) 40.6 (16)	
10	0	1.016 (40)	53.3 (0.0021)	762.0 (300) 889.0 (350) 1016.0 (400)		22.9 (9) 27.9 (11)	
11	0	1.016 (40)	53.3 (0.0021)	1778.0 (700) 1651.0 (650) 1270.0 (500)		35.6 (14) 30.5 (12)	
12***	0	1.016 (40)	53.3 (0.0021)	1905.0 (750) 2036.0 (800) 1905.0 (750)		33.0 (13) 45.7 (18)	
13***	0	1.778 (70)	53.3 (0.0021)	508.0 (200) 254.0 (100) 508.0 (200)		17.8 (7) 30.5 (12)	
14	0	2.540 (100)	53.3 (0.0021)	1524.0 (600) 1016.0 (400) 1016.0 (400)	339, 353	10.2 (4) 102.0 (40)	288, 306
15	0	1.016 (40)	109.2 (0.0043)	1524.0 (600) 1905.0 (750) 1778.0 (700)		55.9 (22) 63.5 (25)	
16	0	1.778 (70)	109.2 (0.0043)	1016.0 (400) 1016.0 (400) 381.0 (150)		53.3 (21) 33.0 (13)	

Table A-1 Continued. Results of Turning Tests*

Order of Cut	SCEA (Degrees)	Depth-Of-Cut (mm; Inch x 10^{-3})	Feedrate (μm/Rev; IPR)	Burr Properties** Height (μm; Inch x 10^{-4})	Hardness (Knoop)	Thickness (μm; Inch x 10^{-4})	Workpiece Hardness (Knoop)
17	0	2.540 (100)	109.2 (0.0043)	109.2 (43) 63.5 (25) 71.1 (28)		30.5 (12) 61.0 (24)	
18	0	1.016 (40)	165.1 (0.0065)	762.0 (300) 254.0 (100) 508.0 (200)		50.4 (20) 61.0 (24)	
19	0	1.778 (70)	165.1 (0.0065)	1270.0 (500) 381.0 (150) 304.8 (120)		25.4 (10) 71.1 (28)	
20	0	2.540 (100)	165.1 (0.0065)	1905.0 (750) 2032.0 (800) 1778.0 (700)	366, 404	142.2 (56) 182.9 (72)	294, 296
21	-17-1/2	1.778 (70)	53.3 (0.0021)	17.8 (7) 12.7 (5) 5.4 (2)		0 (0)	
22***	-17-1/2	1.016 (40)	53.3 (0.0021)	1905.0 (750) 2032.0 (800) 1905.0 (750)		61.0 (24) 76.2 (30)	
23	-17-1/2	1.778 (70)	53.3 (0.0021)	2159.0 (850) 1905.0 (750) 2032.0 (800)		102.0 (40)	295, 276
24	-17-1/2	2.540 (100)	53.3 (0.0021)	1524.0 (600) 1651.0 (650) 1778.0 (700)	304, 325	1651.0 914.4T† (650 360T) 1981.2 1066.8T† (780 420T)	232

Table A-1 Continued. Results of Turning Tests*

Order of Cut	SCEA (Degrees)	Depth-Of-Cut (mm; Inch x 10^{-3})	Feedrate (μm/Rev; IPR)	Burr Properties** Height (μm; Inch x 10^{-4})	Hardness (Knoop)	Thickness (μm; Inch x 10^{-4})	Workpiece Hardness (Knoop)
25	-17-1/2	1.016 (40)	109.2 (0.0043)	3302.0 (1300) 2540.0 (1000) 2032.0 (800)		114.3 (45)	
26	-17-1/2	1.778 (70)	109.2 (0.0043)	1016.0 (400) 889.0 (350) 1016.0 (400)	340, 332	624.8 (246) 561.3 (221)	297
27	17-1/2	1.016 (40)	81.3 (0.0032)	762.0 (300) 1143.0 (450) 1016.0 (400)		106.7 (42) 134.6 (53)	
28	17-1/2	1.016 (40)	81.3 (0.0032)	0 (0) 0 (0) 0 (0)	360, 369	20.3 (8) 0 (0)	314
29	17-1/2	1.778 (70)	81.3 (0.0032)	0 (0) 0 (0) 0 (0)	385, 385	15.2 (6) 0 (0)	295
30	17-1/2	2.540 (100)	81.3 (0.0032)	0 (0) 0 (0) 0 (0)	340, 355		295
31	0	1.016 (40)	81.3 (0.0032)	1270.0 (500) 1270.0 (500) 1270.0 (500)	385, 379	86.4 (34) 50.8 (20)	295
32	0	1.778 (70)	81.3 (0.0032)	127.0 (50) 127.0 (50) 127.0 (50)	393, 385	73.7 (29) 101.6 (40)	290

Table A-1 Continued. Results of Turning Tests*

Order of Cut	SCEA (Degrees)	Depth-Of-Cut (mm; Inch x 10^{-3})	Feedrate (μm/Rev; IPR)	Burr Properties** Height (μm; Inch x 10^{-4})	Hardness (Knoop)	Thickness (μm; Inch x 10^{-4})	Workpiece Hardness (Knoop)
33	0	2.540 (100)	81.3 (0.0032)	762.0 (300) 762.0 (300) 762.0 (300)	333, 354	325.1 101.6T† (128 40T) 274.3 101.6T† (108 40T)	282, 297
34	-17-1/2	1.016 (40)	53.3 (0.0021)	1270.0 (500) 1397.0 (550) 1270.0 (500)	382, 388	106.7 (42) 101.6 (40)	310
35	-17-1/2	1.016 (40)	53.3 (0.0021)	1016.0 (400) 1016.0 (400) 1016.0 (400)	390, 385		295
36	-17-1/2	1.016 (40)	53.3 (0.0021)	1905.0 (750) 1778.0 (700) 1905.0 (750)	390, 382	132.1 (52) 111.8 (44)	295
37	-17-1/2	1.778 (70)	53.3 (0.0021)	1905.0 (750) 1905.0 (750) 1905.0 (750)	340, 380	254.0 (100) 175.3 (69)	305
38	-17-1/2	2.540 (100)	53.3 (0.0021)	2540.0 (1000) 2540.0 (1000) 2540.0 (1000)	344, 366	1473.2 1016.0T† (580 400T) 1600.2 1295.4T† (630 510T)	232
39	-17-1/2	1.016 (40)	81.3 (0.0032)	2540.0 (1000) 2540.0 (1000) 2540.0 (1000)	365,340	132.1 (52) 127.0 (50)	286
40	-17-1/2	1.778 (70)	81.3 (0.0032)	1524.0 (600) 1524.0 (600) 1524.0 (600)	315, 294	375.9 (148) 1016.0 (400)	275

Table A-1 Continued. Results of Turning Tests*

Order of Cut	SCEA (Degrees)	Depth-Of-Cut (mm; Inch x 10^{-3})	Feedrate (μm/Rev; IPR)	Burr Properties** Height (μm; Inch x 10^{-4})	Hardness (Knoop)	Thickness (μm; Inch x 10^{-4})	Workpiece Hardness (Knoop)
41	-17-1/2	2.540 (100)	81.3 (0.0032)	1270.0 (500) 1270.0 (500) 1270.0 (500)	400, 406	1803.4†† (710) 1447.8†† (570)	300, 311
42	-17-1/2	1.016 (40)	109.2 (0.0043)	2540.0 (1000) 2286.0 (900) 2540.0 (1000)	350, 355	61.0 (24) 73.7 (29)	265
43	-17-1/2	1.778 (70)	109.2 (0.0043)	1143.0 (450) 1270.0 (500) 1270.0 (500)	387, 392	248.9 (98) 210.8 (83)	314
44	-17-1/2	2.540 (100)	109.2 (0.0043)	1270.0 (500) 1270.0 (500) 1270.0 (500)	380, 355	1107.4 406.4T† (436 160T) 939.8 (370)	280, 282
45	-17-1/2	1.016 (40)	109.2 (0.0043)	1524.0 (600) 1524.0 (600) 1524.0 (600)	355, 416	891.5 (351) 889.0 (350)	294
46†††	-17-1/2	1.016 (40)	53.3 (0.0021)	1905.0 (750) 1905.0 (750) 1905.0 (750)	370, 370	5.1 (2) 53.3 (21)	268
47†††	0	1.016 (40)	53.3 (0.0021)	381.0 (150) 508.0 (200) 254.0 (100)		81.3 (32)	
48†††	17-1/2	1.016 (40)	53.3 (0.0021)	17.8 (7) 30.5 (12) 17.8 (7)		40.6 (16) 20.4 (8)	

Table A-1 Continued. Results of Turning Tests*

Order of Cut	SCEA (Degrees)	Depth-Of-Cut (mm; Inch x 10^{-3})	Feedrate (μm/Rev; IPR)	Burr Properties** Height (μm; Inch x 10^{-4})	Hardness (Knoop)	Thickness (μm; Inch x 10^{-4})	Workpiece Hardness (Knoop)
49†††	-17-1/2	1.016 (40)	53.3 (0.0021)	2794.0 (1100) 2921.0 (1150) 2794.0 (1100)	321, 323	223.5 101.6T† (88 40T)	294, 302
50††††	17-1/2	1.016 (40)	53.3 (0.0021)	43.2 (17) 17.8 (7) 45.7 (18)	332,350	20.3 (8) 22.9 (9)	265
51††††	17-1/2	1.016 (40)	53.3 (0.0021)	7.6 (3) 7.6 (3) 7.6 (3)		30.5 (12)	
52††††	0	1.016 (40)	53.3 (0.0021)	81.3 (32) 61.0 (24) 99.1 (39)		71.1 (28) 50.8 (20)	
53††††	-17-1/2	1.016 (40)	53.3 (0.0021)	1524.0 (600) 1524.0 (600) 1524.0 (600)	323, 326	71.1 (28)	302, 305

*Workpiece: 303Se stainless steel, 12.7 mm (0.5 inch) in diameter. Speed 1800 rpm. Tool: -35° diamond shape throwaway profiling insert, 5-degree rake unless otherwise noted. Any BUE on tool was removed before making subsequent cuts.

**Multiple entries indicate that more than one measurement was made. Thickness and hardness were measured in metallurgical mounts. Hardness was measured with a 500-g load.

***Although no BUE was visible on the tool, chips indicated that BUE was forming; chips were continuous.

†Burr was triangular at base; first number indicates actual width at base; T indicates the typical, average width.

††Widths were measured at base.

†††Using -15-degree-back-rake insert.

††††Using +15-degree-back-rake insert.

Table A-2. Alias Structure for Fractional Replicate

Equivalents
I = ACD = BDF = AEF = BCE = ABCF = ABDE = CDEF
A = CD = EF = BCF = BDE = ABCE = ABDF = ACDEF
B = CE = DF = ACF = ADE = ABCD = ABEF = BCDEF
C = AD = BE = ABF = DEF = BCDF = ACEF = ABCDE
D = AC = BF = ABE = CEF = ADEF = BCDE = ABCDF
E = AF = BC = ABD = CDF = ACDE = BDEF = ABCEF
F = AE = BD = ABC = CDE = ACDF = BCEF = ABDEF
AB = CF = DE = ADF = BCE = BEF = ACE = ABCDEF

Table A-3. Workpiece-Material Properties

Property	Material				
	Type A*	Type B**	15-5PH	303Se	BeCu
Yield Strength					
MPa	344.7	390.9	1034.1	413.6	654.9
KSI	50.0	56.7	150.0	60.0	95.0
Tensile Strength					
MPa	723.2	390.9	1137.5	1240.9	703.2
KSI	104.9	56.7	165.0	180.0	102.0
Elongation in 50.8 mm or 2 Inches (Percent)	71.5	0.78	16.0	50.0	26.0
Reduction of Area (Percent)		0	58.0	55.0	
Hardness (Brinell 3000 kg)	176	290	352	160	216
Strain-Hardening Exponent	0.42	0	0.08	0.56	0.10
Modulus of Elasticity					
GPA	137.90	206.82	199.93	199.93	127.54
PSI x 10^6	20.0	30.0	29.0	29.0	18.5

*Glass sealing alloy, 53Fe-29Ni-17Co, SAE unified number K94610.
**2V permendur high magnetic permeability steel, 49Fe-49Co-2V, SAE unified number K95100

Table A-4. Average Unit Power

Factor Levels ABCDEF	Tool	Average Unit Power for Indicated Material* ($W/cm^3/s$; $HP/in.^3/min$)				
		303Se	15-5PH	BeCu	TypeA**	Type B***
111111	1	2.94 (3.8720)	1.79 (2.3499)	0.92 (1.2065)	1.54 (2.0202)	3.32 (4.3631)
112222	2	3.63 (4.7699)	2.93 (3.8580)	1.47 (1.9290)	2.11 (2.7708)	4.37 (5.7520)
121122	3	3.31 (4.3490)	2.67 (3.5073)	1.31 (1.7186)	1.92 (2.5253)	4.58 (6.0326)
122211	4	3.82 (5.0224)	2.03 (2.6656)	0.98 (1.2907)	1.58 (2.0833)	2.81 (3.6967)
211212	5	4.48 (5.8922)	2.67 (3.5073)	1.57 (2.0693)	2.56 (3.3670)	8.48 (11.1532)
212121	6	3.16 (4.1526)	1.95 (2.5603)	0.91 (1.1925)	7.92 (10.4167)	3.36 (4.4192)
221221	7	3.63 (4.7699)	2.03 (2.6656)	1.00 (1.3187)	6.94 (2.3148)	3.23 (4.2438)
222112	8	5.86 (7.7160)	2.99 (3.9282)	2.13 (2.8058)	2.40 (3.1566)	5.17 (6.8042)

*Data are an average from ten specimens at each of the indicated levels. See Table 2 in text for explanation of coding.
**Glass sealing alloy, 53Fe-29Ni-17Co, SAE unified number K94610.
***2V permendur high magnetic permeability steel, 49Fe-49Co-2V, SAE unified number K95100.

Table A-5. Average Burr Height

Factor Levels ABCDEF	Average Burr Height for Indicated Material (μm; In. x 10^{-4})				
	303Se	15-5PH	BeCu	Type A*	Type B**
111111	501.7 (197.5)	34.0 (13.4)	52.6 (20.7)	39.4 (15.5)	53.3 (21.4)
112222	384.6 (151.4)	0 (0)	63.0 (24.8)	77.2 (30.4)	20.8 (8.2)
121122	245.6 (96.7)	0 (0)	11.7 (4.6)	68.8 (27.1)	10.7 (4.2)
122211	857.0 (337.4)	90.2 (35.5)	14.5 (5.7)	62.5 (24.6)	59.7 (23.5)
211212	547.1 (215.4)	169.9 (66.9)	70.1 (27.6)	1019.0 (401.2)	22.6 (8.9)
212121	566.2 (222.9)	23.1 (9.1)	42.4 (16.7)	67.8 (26.7)	24.4 (9.6)
221221	509.8 (200.7)	25.9 (10.2)	38.1 (15.0)	105.4 (41.5)	37.8 (14.9)
222112	324.4 (127.7)	23.1 (9.1)	37.1 (14.6)	223.8 (88.1)	13.5 (5.3)

*Glass sealing alloy, 53Fe-29Ni-17Co, SAE unified number K94610.
**2V permendur high magnetic permeability steel, 49Fe-49Co-2V, SAE unified number K95100.

Table A-6. Average Burr Thickness

Factor Levels ABCDEF	Average Burr Thickness for Indicated Material (μm; In. x 10^{-4})				
	303Se	15-5PH	BeCu	Type A*	Type B**
111111	154.4 (60.8)	114.5 (10.7)	78.2 (30.8)	83.6 (32.9)	71.1 (28.0)
112222	115.6 (45.5)	0 (0)	68.1 (26.8)	86.4 (34.0)	27.7 (10.9)
121122	88.4 (34.8)	0 (0)	22.4 (8.8)	80.3 (31.6)	10.2 (4.4)
122211	107.7 (42.4)	72.4 (28.5)	26.9 (10.6)	89.9 (35.4)	81.8 (32.2)
211212	114.0 (44.9)	99.6 (39.2)	70.4 (27.7)	110.2 (43.4)	21.8 (8.6)
212121	133.1 (52.4)	45.0 (17.7)	59.7 (23.5)	78.5 (30.9)	37.1 (14.6)
221221	104.6 (41.2)	55.6 (21.9)	76.5 (30.1)	98.0 (38.6)	52.6 (20.7)
222112	106.9 (42.1)	38.1 (15.0)	48.8 (19.2)	101.6 (40.0)	19.3 (7.6)

*Glass sealing alloy, 53Fe-29Ni-17Co, SAE unified number K94610.
**2V permendur high magnetic permeability stcel, 49Fe-49Co-2V, SAE unified number K95100.

Table A-7. Average Cutting Force F_T

Factor Levels ABCDEF	Average Cutting Force F_T for Indicated Material (N; Pounds)				
	303Se	15-5PH	BeCu	Type A*	Type B**
111111	245.5 (55.2)	149.0 (33.5)	76.5 (17.2)	128.1 (28.8)	276.7 (62.2)
112222	60.5 (13.6)	48.9 (11.0)	24.5 (5.5)	35.1 (7.9)	72.9 (16.4)
121122	53.4 (12.4)	44.5 (10.0)	21.8 (4.9)	32.0 (7.2)	76.5 (17.2)
122211	318.5 (71.6)	169.0 (38.0)	81.8 (18.4)	132.1 (29.7)	234.4 (52.7)
211212	74.7 (16.8)	44.5 (10.0)	26.2 (5.9)	42.7 (9.6)	141.4 (31.8)
212121	263.3 (59.2)	162.4 (36.5)	75.6 (17.0)	132.1 (29.7)	280.4 (63.0)
221221	302.5 (68.0)	169.0 (38.0)	83.6 (18.8)	146.8 (33.0)	269.1 (60.5)
222112	97.9 (22.0)	49.8 (11.2)	35.6 (8.0)	40.0 (9.0)	86.3 (19.4)

*Glass sealing alloy, 53Fe–29Ni–17Co, SAE unified number K94610.
**2V permendur high magnetic permeability steel, 49Fe-49Co-2V, SAE unified number K95100.

Table A-8. Average Cutting Force F_A

Factor Levels ABCDEF	Average Cutting Force F_A for Indicated Material (N; Pounds)				
	303Se	15-5PH	BeCu	Type A*	Type B**
111111	137.9 (31.0)	81.8 (18.4)	23.1 (5.2)	57.4 (12.9)	137.9 (31.0)
112222	31.1 (7.0)	21.8 (4.9)	9.8 (2.2)	16.9 (3.8)	24.0 (5.4)
121122	26.7 (6.0)	18.2 (4.1)	3.6 (1.8)	16.5 (3.7)	33.4 (7.5)
122211	177.9 (40.0)	97.0 (21.8)	35.6 (8.0)	68.5 (15.4)	136.6 (30.7)
211212	44.5 (10.0)	20.9 (4.7)	15.1 (3.4)	25.4 (5.7)	33.8 (7.6)
212121	149.0 (33.5)	74.3 (16.7)	31.1 (7.0)	58.7 (13.2)	124.1 (27.9)
221221	175.7 (39.5)	85.0 (19.1)	36.0 (8.1)	81.8 (18.4)	141.4 (31.8)
222112	36.5 (8.2)	17.8 (4.0)	9.3 (2.1)	20.0 (4.5)	25.4 (5.7)

*Glass sealing alloy, 53Fe-29Ni-17Co, SAE unified number K94610.
**2V permendur high magnetic permeability steel, 49Fe-49Co-2V, SAE unified number K95100.

Table A-9. Constants for Tool-Wear Equations

Material	Factor Levels	Variable and Measuring Units	Constants* a_1	Constants* a_2
15-5PH	122211	F_A (N; Pounds)	80.6 (18.13)	2.98 (0.67)
BeCu	211212	F_A (N; Pounds)	8.9 (2.0)	1.1 (0.25)
Type A**	221221	F_A (N; Pounds)	67.6 (15.2)	2.6 (0.58)
Type A	222112	F_A (N; Pounds)	16.3 (3.67)	0.7 (0.15)
Type B***	111111	F_A (N; Pounds)	114.5 (25.73)	4.3 (0.96)
Type B	121122	F_A (N; Pounds)	21.7 (4.87)	2.1 (0.48)
Type B	221221	F_A (N; Pounds)	125.7 (28.27)	2.8 (0.64)
Type B	222112	F_A (N; Pounds)	20.1 (4.53)	0.9 (0.21)
BeCu	111111	F_T (N; Pounds)	62.6 (14.07)	2.5 (0.57)
BeCu	112222	F_T (N; Pounds)	20.1 (4.53)	0.8 (0.18)
Type B	111111	F_T (N; Pounds)	208.5 (46.87)	12.4 (2.79)
Type B	112222	F_T (N; Pounds)	36.2 (8.13)	6.7 (1.50)
Type B	211212	F_T (N; Pounds)	71.5 (16.07)	12.7 (2.86)
Type B	212121	F_T (N; Pounds)	216.5 (48.67)	11.6 (2.60)
Type B	221221	F_T (N; Pounds)	223.9 (50.33)	8.2 (1.85)
Type B	222112	F_T (N; Pounds)	45.4 (10.20)	7.4 (1.67)
303Se	111111	Burr Thickness (μm; Inch)	53.3 (0.0021)	18.29 (0.00072)

Table A-9 Continued. Constants for Tool-Wear Equations

Material	Factor Levels	Variable and Measuring Units	Constants* a_1	Constants* a_2
303Se	211212	Burr Thickness (μm;Inch)	142.2 (0.0056)	-5.33 (-0.00021)
303Se	221221	Burr Thickness (μm;Inch)	48.3 (0.0019)	10.41 (0.00041)
Type B	121122	Burr Thickness (μm;Inch)	33.0 (0.0013)	-4.06 (-0.00016)
Type B	211212	Burr Thickness (μm;Inch)	83.8 (0.0033)	-11.18 (-0.00044)
Type B	212121	Burr Thickness (μm;Inch)	86.4 (0.0034)	-8.89 (-0.00035)
303Se	221221	Burr Length (μm;Inch)	20.3 (0.0008)	89.15 (0.00351)
15-5PH	212121	Burr Length (μm;Inch)	2.5 (0.0001)	3.81 (0.00015)
Type B	121122	Burr Length (μm;Inch)	33.0 (0.0013)	-4.06 (-0.00016)
Type B	211212	Burr Length (μm;Inch)	83.8 (0.0033)	-11.18 (-0.00044)
Type B	212121	Burr Length (μm;Inch)	55.9 (0.0022)	-5.59 (-0.00022)
Type B	221221	Burr Length (μm;Inch)	53.3 (0.0021)	-2.54 (-0.00010)

*These constants are for use in Equation 17 of this report:

$$Y = a_1 + a_2\left(\frac{L}{5.625}\right),$$

where L is the axial length-of-cut in inches and Y is the dependent variable (force or burr size in indicated unit of measure).

**Glass sealing alloy, 53Fe-29Ni-17Co, SAE unified number K94610.

***2V permendur high magnetic permeability steel, 49Fe-49Co-2V, SAE unified number K95100.

DISTRIBUTION

	Copy
R. Bulcock, ERDA-KCAO, 1D49	1
J. E. Green, G. E. Pinellas	2
J. W. Baker, Rocky Flats	3
K. Thistlewood, Rocky Flats	4
G. P. Ford, SLA	5
K. Gillespie, SLA	6
R. S. Pinkham, SLA	7
A. L. Thornton, SLA	8
W. A. Johaningsmeir, D/231, 1D40	9
H. L. Price, D/261, FU34	10
E. L. Young, D/261, FU34	11
B. J. Neal, D/411, 2E29	12
J. M. Lowrey, D/415, 2B30	13
H. T. Barnes, D/554, BD50	14
J. D. Corey, D/554, BD50	15-16
L. Stratton, D/554, 2C44	17-19
E. F. Felkner, D/752, 1A41	20
J. D. Johnson, D/752, 1A41	21
R. F. Cell, D/755, 1A42	22
R. P. Frohmberg, D/800, 2A39	23
J. A. Knuth, D/800/D. D. Oswald/J. P. Dycus/ D. R. Wachter, D/822, 2A36	24
J. L. Couchman/F. J. Boyle/B. W. Landes, D/821, 2A36	25
R. K. Albright, D/822, 2A36	26
L. K. Gillespie, D/822, 2A36	27-43
G. E. Klement, D/822, 2A36	44
W. P. McKay, D/822, 2A36	45
D. P. Roberts/C. E. Spitzkeit, D/823, 2A36	46
R. W. Lange, D/861, 2A31	47
R. E. Kessler, D/865, 2C40	48

BDX-613-1748 (Rev.)

BURRS PRODUCED BY TURNING, L. K. Gillespie, Topical, December 1978

Methods were determined for controlling turning-burr size to reduce deburring cost and improve the quality of miniature precision components. A maximum burr height and thickness of 25.4 μm (0.001 inch) are essential to obtaining consistent deburring and limiting stock loss to 2.54 μm (0.0001 inch) and edge radii to 76.4 μm (0.003 inch). Controlling factors include the tool's side-cutting edge angle, back rake,

MECHANICAL: Turning Burrs

BURRS PRODUCED BY TURNING, L. K. Gillespie, Topical, BDX-613-1748 (Rev.), December 1978.

Methods were determined for controlling turning-burr size to reduce deburring cost and improve the quality of miniature precision components. A maximum burr height and thickness of 25.4 μm (0.001 inch) are essential to obtaining consistent deburring and limiting stock loss to 2.54 μm (0.0001 inch) and edge radii to 76.4 μm (0.003 inch). Controlling factors include the tool's side-cutting edge angle, back rake,

BURRS PRODUCED BY TURNING, L. K. Gillespie, Topical, BDX-613-1748 (Rev.), December 1978

Methods were determined for controlling turning-burr size to reduce deburring cost and improve the quality of miniature precision components. A maximum burr height and thickness of 25.4 μm (0.001 inch) are essential to obtaining consistent deburring and limiting stock loss to 2.54 μm (0.0001 inch) and edge radii to 76.4 μm (0.003 inch). Controlling factors include the tool's side-cutting edge angle, back rake,

feedrate, and radial depth-of-cut, and the material's strain-hardening exponent and ductility.

feedrate, and radial depth-of-cut, and the material's strain-hardening exponent and ductility.

feedrate, and radial depth-of-cut, and the material's strain-hardening exponent and ductility.